**Atmospheric
Chemistry
and Physics**

Future impact of non-land based traffic emissions on atmospheric ozone and OH – an optimistic scenario and a possible mitigation strategy

Ø. Hodnebrog[1,*], T. K. Berntsen[1], O. Dessens[2,**], M. Gauss[1,3], V. Grewe[4], I. S. A. Isaksen[1], B. Koffi[5], G. Myhre[6], D. Olivié[7,***], M. J. Prather[8], J. A. Pyle[2], F. Stordal[1], S. Szopa[5], Q. Tang[8], P. van Velthoven[9], J. E. Williams[9], and K. Ødemark[1]

[1]Department of Geosciences, University of Oslo, Norway
[2]Centre for Atmospheric Science, Department of Chemistry, Cambridge, UK
[3]Norwegian Meteorological Institute, Oslo, Norway
[4]Deutsches Zentrum für Luft- und Raumfahrt, Institut für Physik der Atmosphäre, Oberpfaffenhofen, Germany
[5]Laboratoire des Sciences du Climat et de l'Environment (LSCE-IPSL), Gif-sur-Yvette, France
[6]Center for International Climate and Environmental Research-Oslo (CICERO), Oslo, Norway
[7]Centre National de Recherches Météorologiques GAME/CNRM (Météo-France, CNRS), Toulouse, France
[8]Department of Earth System Science, University of California, Irvine, USA
[9]Royal Netherlands Meteorological Institute, KNMI, De Bilt, The Netherlands
[*]now at: CICERO, Oslo, Norway
[**]now at: UCL Energy Institute, University College London, London, UK
[***]now at: Department of Geosciences, University of Oslo, Norway and CICERO, Oslo, Norway

Abstract. The impact of future emissions from aviation and shipping on the atmospheric chemical composition has been estimated using an ensemble of six different atmospheric chemistry models. This study considers an optimistic emission scenario (B1) taking into account e.g. rapid introduction of clean and resource-efficient technologies, and a mitigation option for the aircraft sector (B1 ACARE), assuming further technological improvements. Results from sensitivity simulations, where emissions from each of the transport sectors were reduced by 5 %, show that emissions from both aircraft and shipping will have a larger impact on atmospheric ozone and OH in near future (2025; B1) and for longer time horizons (2050; B1) compared to recent time (2000). However, the ozone and OH impact from aircraft can be reduced substantially in 2050 if the technological improvements considered in the B1 ACARE will be achieved.

Shipping emissions have the largest impact in the marine boundary layer and their ozone contribution may exceed 4 ppbv (when scaling the response of the 5 % emission perturbation to 100 % by applying a factor 20) over the North Atlantic Ocean in the future (2050; B1) during northern summer (July). In the zonal mean, ship-induced ozone relative to the background levels may exceed 12 % near the surface. Corresponding numbers for OH are 6.0×10^5 molecules cm^{-3} and 30 %, respectively. This large impact on OH from shipping leads to a relative methane lifetime reduction of 3.92 ($\pm$0.48) % on the global average in 2050 B1 (ensemble mean CH$_4$ lifetime is 8.0 ($\pm$1.0) yr), compared to 3.68 ($\pm$0.47) % in 2000.

Aircraft emissions have about 4 times higher ozone enhancement efficiency (ozone molecules enhanced relative to NO$_x$ molecules emitted) than shipping emissions, and the maximum impact is found in the UTLS region. Zonal mean aircraft-induced ozone could reach up to 5 ppbv at northern mid- and high latitudes during future summer (July 2050; B1), while the relative impact peaks during northern winter (January) with a contribution of 4.2 %. Although the aviation-induced impact on OH is lower than for shipping, it still causes a reduction in the relative methane lifetime of 1.68 ($\pm$0.38) % in 2050 B1. However, for B1 ACARE the perturbation is reduced to 1.17 ($\pm$0.28) %, which is lower than the year 2000 estimate of 1.30 ($\pm$0.30) %.

Based on the fully scaled perturbations we calculate net radiative forcings from the six models taking into account

---

ozone, methane (including stratospheric water vapour), and methane-induced ozone changes. For the B1 scenario, shipping leads to a net cooling with radiative forcings of -28.0 (± 5.1) and -30.8 (± 4.8) mW m^{-2} in 2025 and 2050, respectively, due to the large impact on OH and, thereby, methane lifetime reductions. Corresponding values for the aviation sector shows a net warming effect with 3.8 (± 6.1) and 1.9 (± 6.3) mW m^{-2}, respectively, but with a small net cooling of -0.6 (± 4.6) mW m^{-2} for B1 ACARE in 2050.

1 Introduction

Increasing population and economic turnover will lead to increasing transport demand notably for aviation (AIR) and maritime shipping (SHIP). This will outpace technological improvements and lead to increasing emissions of various air pollutants, affecting air quality and climate through a complex system of chemical reactions and aerosol interactions. From a climate perspective, the present (2000) impact on radiative forcing (RF) is positive for AIR and negative for SHIP (Fuglestvedt et al., 2008; Balkanski et al., 2010), mostly due to formation of contrail cirrus in the first and sulphate in the latter. A first estimate of aircraft-induced cloudiness based on a climate model study was just recently given (Burkhardt and Karcher, 2011), however, the magnitude of positive RF from contrail cirrus is under debate (Lee et al., 2010). Substantial contributions also stem from the emissions of nitrogen oxides (NO$_x$), carbon monoxide (CO) and non-methane hydrocarbons (NMHCs). These relatively short-lived gases change the oxidative state of the atmosphere and tend to give a positive radiative forcing through the increase in ozone (e.g. Ramanathan and Dickinson, 1979; Berntsen et al., 1997), while enhanced OH levels are known to reduce the lifetime of methane (CH$_4$) and thereby cause negative RF (e.g. Crutzen, 1987; Shindell et al., 2005). Among the various transport sectors, previous studies have shown that the warming effect is most efficient (relative to the number of NO$_x$ molecules emitted) for AIR (e.g. Fuglestvedt et al., 2008) because changes in ozone have their largest impact on climate when they occur in the UTLS (upper troposphere/lower stratosphere) region, due to the low temperatures found near the tropopause (Wang and Sze, 1980; Lacis et al., 1990; Hansen et al., 1997). On the other hand, the cooling effect caused by changes in methane lifetimes dominates the SHIP impact (e.g. Myhre et al., 2011) because of the large amounts of NO$_x$ emitted into the clean maritime boundary layer. Due to the different effects on the atmospheric composition, it is important to study the AIR and SHIP sectors individually, especially when it comes to initiating mitigation measures. Another important aspect regarding non-land based traffic emissions, as opposed to land based traffic emissions, is the fact that the background conditions are usually relatively clean

and this is known to increase the enhancement efficiencies of ozone and OH (e.g. Hoor et al., 2009).

IPCC (1999) published an assessment of the impact of aviation on climate, which was later updated by Sausen et al. (2005), and recently by Lee et al. (2009). Several other studies have also investigated how aircraft NO$_x$ emissions alter the chemical composition of the atmosphere (e.g. Hidalgo and Crutzen, 1977; Johnson et al., 1992; Brasseur et al., 1996; Schumann, 1997; Grewe et al., 1999, 2007; Schumann et al., 2000; Kraabøl et al., 2002; Stevenson et al., 2004; Gauss et al., 2006; Søvde et al., 2007). The studies dealing with impact from future subsonic aircraft NO$_x$ emissions project an increase in aircraft-induced ozone in 2050 compared to the present day atmosphere, but the effect depends on the emission scenario used. Søvde et al. (2007) estimated a maximum zonal mean aircraft-induced ozone increase of about 10 ppbv in the UTLS region for 2050 (annual mean) (aircraft NO$_x$ emissions of 2.18 TgN yr^{-1}). In another study, Grewe et al. (1999) calculated 7 to 10 % increased ozone mixing ratios due to aviation for the same year and region, but for two different emission scenarios (aircraft NO$_x$ emissions of 2.15 and 3.42 TgN yr^{-1}, respectively).

Among the studies on impacts from ship emissions (e.g. Lawrence and Crutzen, 1999; Corbett and Koehler, 2003; Endresen et al., 2003, 2007; Eyring et al., 2005, 2007; Dalsøren and Isaksen, 2006; Dalsøren et al., 2009, 2010), only one has made future projections with atmospheric chemistry models (Eyring et al., 2007). They estimate maximum near-surface ozone contributions from shipping of 5–6 ppbv (annual mean) in the North Atlantic for the year 2000, increasing to 8 ppbv in one of the 2030 scenarios (ship NO$_x$ emissions of 3.10 and 5.95 TgN yr^{-1}, respectively). In a second 2030 scenario the ship emissions were assumed to stabilize at 2000 levels, but the higher background NO$_x$ levels caused a slight decrease in the ozone impact from shipping.

The present study is performed within the EU project QUANTIFY (Quantifying the Climate Impact of Global and European Transport Systems), which was the first attempt of investigating the global scale impact on the atmospheric composition due to emissions from each of the transport sectors. Fuglestvedt et al. (2008) investigated the climate forcing from the transport sectors for year 2000, and later Skeie et al. (2009) estimated transport-induced RF for future scenarios. A multi-model study of the year 2000 impact of transport emissions on the atmospheric chemical composition was performed by Hoor et al. (2009) using the preliminary QUANTIFY emissions. They found a maximum ozone increase from aircraft of 3.69 ppbv in the upper troposphere between 30 and 60° N, and they also found that shipping emissions contributed the most to ozone perturbations in the lower troposphere with around 50 % of the total traffic induced perturbation. The RF results from Hoor et al. (2009) were recently updated by Myhre et al. (2011) who used the final version of the QUANTIFY emissions data to estimate the year 2000 impact. The future impacts of both the

Table 1. Global annual emissions of NO_x, CO and NMHC provided by QUANTIFY (http://www.ip-quantify.eu) for the years 2000, 2025 and 2050 in the B1 scenario. The 2000 emissions are from the final QUANTIFY dataset and thereby differ from the preliminary emissions used in Hoor et al. (2009).

Source	NO_x emissions in Tg(N)			CO emissions in Tg(C)			NMHC emissions in Tg(C)		
	2000	2025B1	2050B1	2000	2025B1	2050B1	2000	2025B1	2050B1
Aircraft	0.85	1.18/1.13*	1.04/0.79*	–	–	–	–	–	–
Ship	4.56	4.93	5.05	0.6	1.0	1.5	0.36	0.51	0.63
Road	8.89	3.29	0.52	47.2	14.8	1.7	11.37	2.74	0.53
Non-traffic	28.9	30.8	31.4	365.3	220.5	196.5	108.1	108.4	109.0
Biogenic, soil	6.89	6.89	6.89	48.2	48.2	48.2	340.5	340.5	340.5

* B1 ACARE aircraft emissions.

emissions and climate changes on transport-induced ozone have so far only been studied by Koffi et al. (2010), using the climate-chemistry model LMDz-INCA (also used in this study). Cariolle et al. (2009) investigated the effect of including an aircraft plume parameterization in large-scale atmospheric models, and similarly the inclusion of a ship plume parameterization was studied by Huszar et al. (2010). Both studies suggested significant reductions in non-land based traffic-induced ozone when plume processes were taken into account. Main results obtained in QUANTIFY are summarized in Lee et al. (2010) (aviation), Eyring et al. (2010) (shipping), and Uherek et al. (2010) (land transport).

The objective of this study is to investigate how emissions from the non-land based traffic sectors (AIR and SHIP) impact atmospheric ozone, OH, and the resulting RF, if precursor emissions from all sectors show reductions due to environmental concerns leading to improved technology. The effects of possible future high emission scenarios will be dealt with in a follow-up study, using the same set of atmospheric chemistry models. The scenarios selected for this purpose are the SRES (Special Report on Emission Scenarios) optimistic B1 and pessimistic A1B (Nakicenovic et al., 2000), respectively, whereas results from the first are presented in this study. As the B1 scenario is considered to be far more optimistic than the A1B scenario (both for transport and non-transport emissions), due to assumptions of e.g. rapid introduction of clean and resource-efficient technologies in the first, the combined results represent possible low or high developments, respectively, of the transport-induced impact on the atmospheric chemical composition, taking into account uncertainties related to the evolution of e.g. economy and technology. More specifically, the B1 scenario is characterized by environmental concerns leading to improved NO_x technology and a relatively smooth transition to alternative energy systems, but without assumptions of climate policies (in accordance with the SRES terms of reference) (Nakicenovic et al., 2000). We have also studied the effect of utilizing additional technological improvements to the aircraft through the B1 ACARE mitigation option (Owen et

al., 2010). The fuel efficiency improvements in B1 ACARE probably require the technology to be driven by concerns over climate change and is thus considered a mitigation scenario. In the following we describe the simulation setup and the emission scenarios (Sect. 2), before giving a short presentation of each of the models in the ensemble (Sect. 3). The impacts on ozone and OH are dealt with in Sects. 4 and 5, respectively, while global radiative forcing calculations are presented in Sect. 6. Finally, our conclusions are given in Sect. 7.

2 Emissions and simulation setup

Traffic emissions of the ozone precursors NO_x, CO and NMHC have been developed for year 2000 and for future scenarios through QUANTIFY (data can be downloaded from www.ip-quantify.eu). Anthropogenic emissions from non-traffic sources were taken from the EDGAR3.2-FT2000 inventory (Olivier et al., 2005; van Aardenne et al., 2005) for year 2000, while the future non-traffic emissions evolve according to the IPCC (Intergovernmental Panel on Climate Change) SRES (Nakicenovic et al., 2000) B1 scenario. Table 1 lists the global annual emissions used in this study, and Fig. 1 shows the time development of NO_x emissions from different transport sectors and for several scenarios. Although the future increase in the global NO_x emissions from AIR and SHIP is relatively small for the B1 scenario, important changes in the regional distribution of emissions can be seen for these transport sectors (Figs. 2–4).

New aircraft emissions scenarios have been developed using the FAST model and are described in Owen et al. (2010). B1 ACARE is a mitigation scenario for aviation and contains additional emission reductions on top of the reductions that are assumed in the B1 scenario. B1 ACARE can be seen as a very optimistic, but feasible, scenario due to concern over climate change. The traffic demand is the same in both scenarios, but excellent fuel efficiency and NO_x improvements are assumed in the mitigation scenario, in accordance with the targets set by the Advisory Council for

Aeronautical Research in Europe (ACARE, 2002). Consequently, the B1 ACARE scenario has 4 and 24 % lower aircraft NO_x emissions than B1 in 2025 and 2050, respectively, and the emissions for 2050 are even lower than the year 2000 estimate. Figure 2 shows that the increase in Europe and Asia in 2025 is smaller for B1 ACARE compared to the B1 scenario, and the emission reductions over the US are stronger in the first scenario. When comparing 2050 with 2025, only a few flight routes have increased emissions in B1 ACARE, and major emission reductions can be seen in Europe, the US, and Japan. The dependency of aircraft NO_x emissions on different latitude intervals can be seen in Fig. 4.

Shipping emissions are based on Endresen et al. (2007) (year 2000) and Eide et al. (2007) (years 2025 and 2050), and are characterized by increased NO_x emissions in the future, even for the optimistic B1 scenario. Already in 2025 the shipping sector could have become the largest emitter of NO_x among the three transport sectors (Fig. 1). Most of the increase for the B1 scenario is distributed among 12 new shipping routes (Fig. 3) that are predicted by Eide et al. (2007). It is worth noting the Northern Sea Route which has increasing emissions from 2000 to 2025, and then shows a slight decline from 2025 to 2050.

Emissions from road transport are based on Borken et al. (2007). Future emissions are documented in Uherek et al. (2010). While road traffic was the dominating source of NO_x emissions among the transport sectors in 2000, assumptions of stricter vehicle emission standards and improvements in technology will lead to a substantial decrease of NO_x emissions in the future scenarios (Fig. 1), particularly for B1. Technology with low NO_x emissions is already available for the road sector, and is faster to implement than for aircraft and shipping as the lifetime of vehicles is shorter. Koffi et al. (2010) showed that the rapid decline in NO_x emissions from road transport will lead to a drastic decrease in the ozone impact of road emissions in 2050. For this reason the impact of road traffic on ozone and OH has not been dealt with in this study, but model results from a policy failure scenario (A1B HIGH) for the road transport sector are subject of a follow-up study.

Additional emissions used in this study include biogenic emissions of isoprene and NO from soils (Jöckel et al., 2006), lightning NO_x emissions specified at 5 $TgN\,yr^{-1}$ (Schumann and Huntrieser, 2007), and biomass burning emissions based on monthly mean Global Fire Emissions Database (GFED) estimates for 2000 (van der Werf et al., 2006) with multiyear (1997–2002) averaged activity data using emission factors from Andreae and Merlet (2001). The biogenic and soil emissions are fixed using the climatology described in Hoor et al. (2009).

Regarding methane, all models used prescribed surface boundary conditions with global CH_4 abundances taken from IPCC (2001), but with a hemispheric scaling such that the mixing ratios were approximately 5 % higher in the Northern than the Southern Hemisphere. Two of the
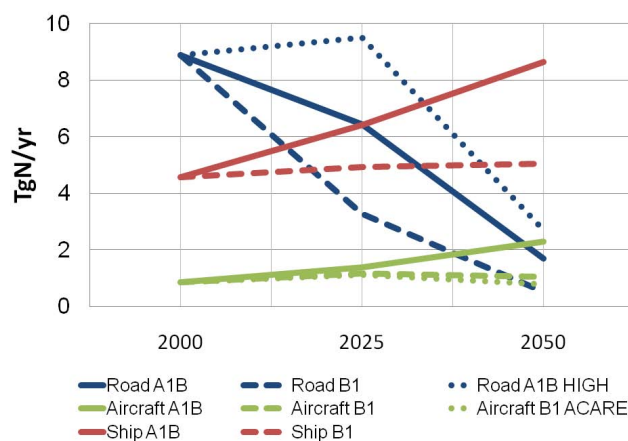

Fig. 1. Time development of NO_x emissions from different transport sectors in the SRES A1B and B1 scenarios, together with the alternative scenarios B1 ACARE and A1B HIGH (unit: $TgN\,yr^{-1}$).

models (p-TOMCAT and MOCAGE) used the IPCC (2001) value for 2000 (1760 ppbv) in all simulations, while the other four models (TM4, OsloCTM2, LMDz-INCA and UCI CTM) updated to the 2025B1 and 2050B1 values (1909 and 1881 ppbv, respectively) in the future simulations. The effect of using 2000 rather than 2025B1 surface methane in the future 2025B1 simulations has been investigated with the OsloCTM2 model and found to have a small impact (up to 1–2 %) on aircraft- and ship-induced relative methane lifetime changes, and on global distributions of ozone and OH perturbations.

The global models included in the ensemble have been run with year 2000 emissions and with the future emission scenarios B1 and B1 ACARE for the years 2025 and 2050. For the year 2000 and for the future B1 simulations, a reference run (BASE) and perturbation runs, one for aircraft (AIR) and one for ship (SHIP), have been performed by each model for each year. For the future B1 ACARE simulations, new reference runs and new aircraft perturbation runs were required in order to study the atmospheric chemistry impact of aircraft emissions under this scenario. In the perturbation simulations, a 5 % reduction has been applied to all emitted species of the respective traffic sector. The reasons not to switch off the emissions in the various transport sectors completely are both to reduce non-linearities in chemistry, and because the unscaled response (i.e. impacts due to 5 % emission perturbation) of the chemical system is expected to be closer to the effect of realistic emission changes than a total removal of the emissions (Hoor et al., 2009). The 5 % reduction approach was used to derive the sensitivity of the atmospheric chemical composition, e.g. ozone concentration, to an emission category with an appropriate accuracy (Hoor et al., 2009). The effect of, e.g. road traffic emissions is obtained by multiplying this sensitivity, e.g. change in ozone concentration per kg emission from road traffic, with the total road traffic

2025-2000   **2050-2025**
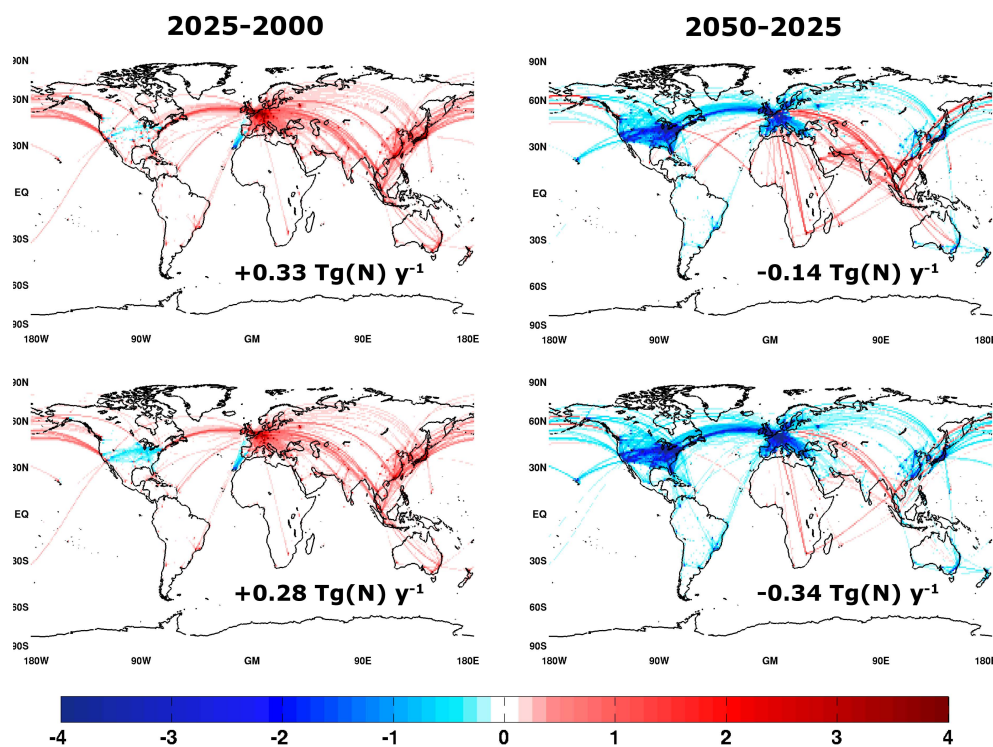
Fig. 2. Spatial distribution of the absolute difference in NO_x emission flux from aircraft for the B1 (top) and B1 ACARE (bottom) scenarios (unit: 10^{13} Δmolecules NO_2 m^{-2} s^{-1}) used in QUANTIFY.

2025-2000   **2050-2025**
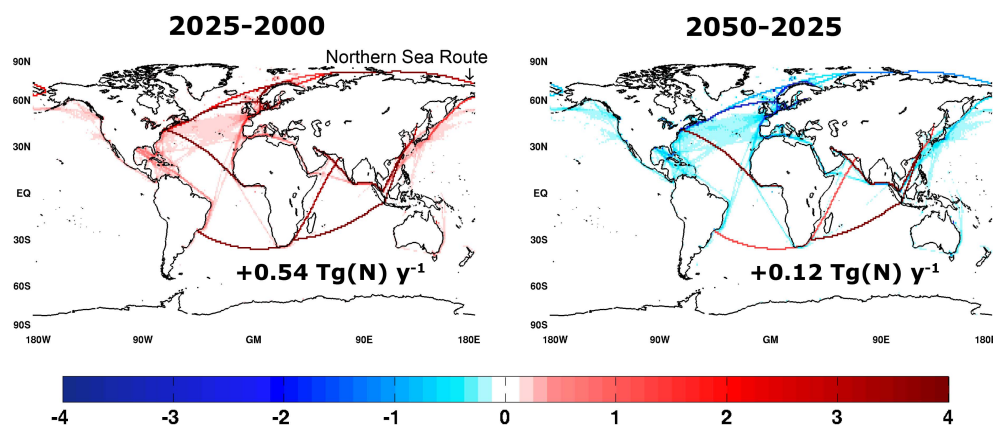
Fig. 3. Spatial distribution of the absolute difference in NO_x emission flux from shipping for the B1 scenario (unit: 10^{13} Δmolecules NO_2 m^{-2} s^{-1}) used in QUANTIFY.

emissions. When comparing results from this study with other studies, it is important to note that the 5 % perturbation approach is very different from removing an emission source by 100 %. Non-linearities in chemistry can lead to large differences between the two approaches as described in Hoor et al. (2009) and Koffi et al. (2010). For further discussions on the small perturbation approach, the reader is referred to Grewe et al. (2010) who state that the method of perturbing an emission source by a small amount (e.g. 5 %), in order to

derive its sensitivity, is well suited to address impacts of e.g. future emission policies. In order to simplify the comparison with Hoor et al. (2009) and Myhre et al. (2011), the ozone and OH results (Sects. 4 and 5.1) are shown unscaled (i.e. the direct difference between BASE-AIR and BASE-SHIP), while calculations of methane lifetime changes and radiative forcings (Sects. 5.2 and 6) have been scaled to 100 % by multiplying the impacts caused by the 5 % emission perturbation with 20 (i.e. 20 × (BASE-AIR) and 20 × (BASE-SHIP)).

Table 2. Specifications of the participating models in this study (modified from Hoor et al., 2009).

Model	TM4	p-TOMCAT	OsloCTM2	LMDz-INCA	UCI CTM	MOCAGE
Operated	KNMI	UCAM-DCHEM	UiO	LSCE	UCI	Météo-France
Model type	CTM	CTM	CTM	CCM (nudged)	CTM	CTM
Meteorology	ECMWF OD	ECMWF OD	ECMWF OD	ECMWF OD	ECMWF OD	ECMWF OD
Hor. resolution	$2° \times 3°$	T21	T42	$3.75° \times 2.5°$	T42	T21
Levels	34	31	60	19	40	60
Model top (hPa)	0.1	10	0.1	3	2	0.1
Transport scheme	Russell and Lerner (1981)	Prather (1986)	Prather (1986)	van Leer (1977)	Prather (1986)	Williamson and Rasch (1989)
Convection	Tiedtke (1989)	Tiedtke (1989)	Tiedtke (1989)	Emanuel (1991, 1993)	Tiedtke (1989)	Bechtold et al. (2001)
Lightning	Meijer et al. (2001)	Price and Rind (1992)	Price and Rind (1992)	Price and Rind (1992), modified	Price and Rind (1992)	Climatology
Transp. species	26	35	76	66	28	65
Total species	42	51	98	96	38	82
Gas phase reactions	68+16	112+27	163+47	291+51	90+22	186+47
Het. Reactions	2	1	7	4	0	9
Strat. chemistry	no	no	yes	no	LINOZ	yes
NMHC chemistry	yes, CBM4	yes	yes	yes	yes	yes
Lightning NO_x (TgN yr^{-1})	5	5	5	2	5	5
References	Williams et al. (2010)	O'Connor et al. (2005)	Gauss et al. (2003), Søvde et al. (2008)	Hauglustaine et al. (2004), Folberth et al. (2006)	Wild et al. (2003), Hsu et al. (2005)	Teyssèdre et al. (2007)

3 Model descriptions

An ensemble of six models has been applied in order to estimate the future impact of non-land based traffic emissions on atmospheric ozone and OH, when considering optimistic scenarios. For the results presented in Sects. 4–6, equally weighted average values of the six models are shown along with the standard deviations, representing the spread in the model results (selected individual model results are shown in Appendix B). Five global Chemistry Transport Models (CTMs) were driven by operational meteorological data from the European Centre for Medium-Range Weather Forecasts (ECMWF) and updated every 6 h (TM4, p-TOMCAT, OsloCTM2, UCI CTM and MOCAGE), while one Climate Chemistry Model (CCM) was nudged towards the ECMWF data (LMDz-INCA). In all simulations the meteorological data are from year 2003 while 2002 data were used to spin-up the models. General model properties are synthesized in Table 2, and short descriptions are given below.

The models have been evaluated by Schnadt et al. (2010) who compared simulated CO to aircraft measurements from 2003, and found underestimation of tropospheric CO at northern hemispheric middle and subtropical latitudes. The discrepancies were possibly related to the biomass burning emissions which were abnormally high in 2003 (e.g. Yurganov et al., 2005), while biomass burning emissions from 2000 were used in the simulations. Comparisons of the annual cycle of ozone from multi-year sonde observations and from the six models are shown in Appendix A (Fig. A1). Overall, the ensemble mean of the model results agrees relatively well with the observations.

3.1 TM4

TM4 is a global chemistry transport model with a horizontal resolution of $3° \times 2°$ and 34 vertical layers up to 0.1 hPa. The version used here has been comprehensively described in

Williams et al. (2010). The chemical scheme is the modified CBM4 mechanism decribed by Houweling et al. (1998), supplemented with sulphur chemistry and with the chemical reaction data being updated by Williams and van Noije (2008). The advection scheme is the slopes method developed by Russell and Lerner (1981), while convection is based on the Tiedtke mass flux scheme (Tiedtke, 1989).

3.2 p-TOMCAT

The global offline chemistry transport model p-TOMCAT is an updated version (see O'Connor et al., 2005) of a model previously used for a range of tropospheric chemistry studies (Law et al., 1998, 2000; Savage et al., 2004). The model is used here with a horizontal resolution of $5.6° \times 5.6°$ (T21) and extends from the surface to 10 hPa in 31 vertical levels. The chemical mechanism includes the reactions of methane, ethane and propane plus their oxidation products and of sulphur species. The model chemistry uses the atmospheric chemistry integration package ASAD (Carver et al., 1997) and is integrated with the IMPACT scheme of Carver and Stott (2000). The chemical rate coefficients used by p-TOMCAT are taken from the IUPAC summary of March 2005. The Prather (1986) scheme is used for advection while convective transport is based on the mass flux parameterization of Tiedtke (1989).

3.3 OsloCTM2

The OsloCTM2 chemistry transport model is used here with both tropospheric and stratospheric chemistry (Gauss et al., 2003; Søvde et al., 2008). It extends from the surface to 0.1 hPa in 60 vertical layers and a horizontal resolution of Gaussian T42 ($2.8° \times 2.8°$) is used. Advection in OsloCTM2 is done using the second order moment scheme (Prather, 1986), while convection is based on the Tiedtke mass flux scheme (Tiedtke, 1989). The Quasi Steady-State Approximation (Hesstvedt et al., 1978) is used for the numerical
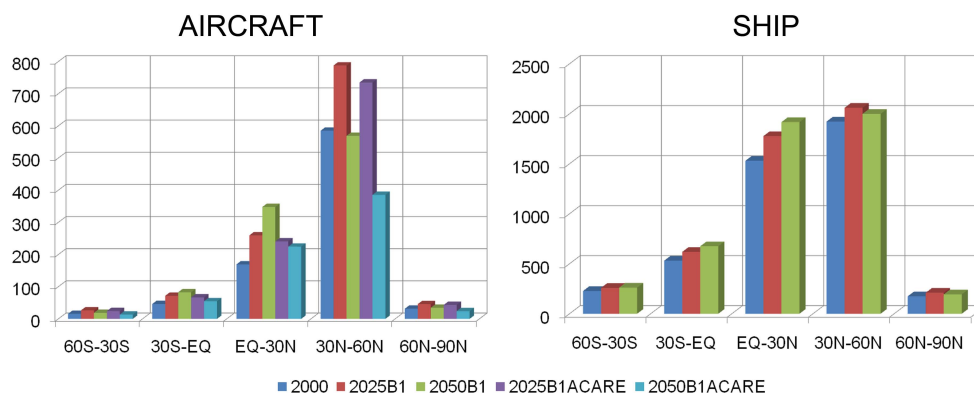
Fig. 4. NO_x emissions $(Gg(N) \, yr^{-1})$ from aircraft (left) and shipping (right) for different latitude intervals and for different years/scenarios. Note that $90°$ S–$60°$ S is not shown in the figures because the emissions in this region are close to zero.

solution in the chemistry scheme, and photodissociation is done on-line using the FAST-J2 method (Wild et al., 2000; Bian and Prather, 2002).

3.4 LMDz-INCA

The LMDz-INCA model consists of the LMDz General Circulation Model (Le Treut et al., 1998), coupled on-line with the chemistry and aerosol model INCA (Folberth et al., 2006). The version 4.0 of the LMDz model has 19 hybrid levels on the vertical from the ground to 3 hPa and a horizontal resolution of $2.5°$ in latitude and $3.75°$ in longitude. The large-scale advection of tracers is performed using the finite volume transport scheme of Van Leer (1977), as described in Hourdin and Armengaud (1999). The turbulent mixing in the planetary boundary layer is based on a second-order closure model. The INCA model considers the surface and 3-D emissions, calculates dry deposition and wet scavenging rates, and integrates in time the concentration of atmospheric species with a time step of 30 min. The CH_4-NO_x-CO-O_3 photochemistry, as well as the oxidation pathways of non-methane hydrocarbons and non-methane volatile organic compounds are taken into account. The winds and temperature predicted by LMDz have been nudged to 6-hourly ECMWF data over the whole model domain with a relaxation time of 2.5 h (Hauglustaine et al., 2004).

3.5 UCI CTM

In this study, the University of California, Irvine (UCI) chemistry transport model extends from the surface to 2 hPa with 40 vertical layers and is run at T42 horizontal resolution. The UCI CTM contains separate tropospheric and stratospheric chemistry. The tropospheric chemistry is simulated by the ASAD (A Self-contained Atmospheric chemistry coDe) software package (Carver et al., 1997) with UCI updates (Tang and Prather, 2010), which include the chemical kinetics and photochemical coefficients from the JPL publication 06–2

(Sander et al., 2006), and quasi steady-state initial guesses for radicals, and $O(^1D)$ included with O_3. The stratospheric chemistry uses the linearized ozone scheme (Linoz), which can include up to four independent species (e.g. O_3, N_2O, NO_y, CH_4), but in this case consists only ozone (Prather and Hsu, 2010). The tropopause, the boundary between the troposphere and the stratosphere, is determined by an artificial tracer (e90) (Prather et al., 2011; Tang et al., 2011). The advection and convection use the same schemes as OsloCTM2.

3.6 MOCAGE

The MOCAGE chemistry transport model is used here with a horizontal resolution of $5.6° \times 5.6°$ (T21) and 60 levels up to 0.1 hPa (Teyssèdre et al., 2007). The chemical scheme is a combination of the tropospheric RELACS scheme (Crassier et al., 2000) (a reduced version of the RACM scheme, Stockwell et al., 1997) and of the stratospheric REPROBUS scheme (Lefèvre et al., 1994) including the heterogeneous chemistry described in Luo et al. (1995). The large-scale transport of the tracers is done using a semi-Lagrangian transport scheme (Williamson and Rasch, 1989), while the convective transport is as described in Bechtold et al. (2001).

4 Ozone

The 2050 B1 annual mean ozone column response to a 5 % perturbation in emissions is shown in Fig. 5 for the aircraft and shipping sectors. The ozone impact from AIR is zonally well mixed, and mostly confined to the Northern Hemisphere (NH) in accordance with the latitudinal distribution of emissions shown in Fig. 4. A method to estimate the contribution of a source is to estimate the sensitivity (ozone change per emission) with a 5 %-perturbation and then to multiply it with the total emission of the source category (e.g. AIR), which effectively equals a scaling of impacts to 100 % by multiplying the response of the 5 % emission perturbation by
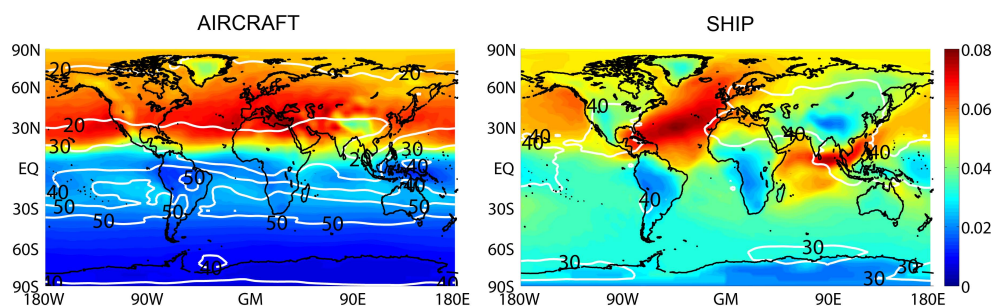
Fig. 5. Yearly mean perturbations of the ozone column (ΔDU, up to 40 hPa) due to a 5 % perturbation of aircraft emissions (left) and ship emissions (right) for the 2050 B1 scenario. The white contour lines show the standard deviation relative to the ensemble mean column perturbation (%), and have been smoothed to improve readability.

20 (Grewe et al., 2010). The results show a maximum ozone column response of 1.6 DU. The corresponding perturbation for SHIP is also 1.6 DU, but much less homogeneously distributed with maximum values occurring over the North Atlantic Ocean and at the coastal areas of South East Asia. These two areas were also identified as peaks in the 2030 model simulations performed by Eyring et al. (2007), who attributed the increased ship-induced tropospheric ozone column over the Indian Ocean to the higher tropopause and more effective vertical transport found there.

Figure 5 also shows the relative standard deviation which represents the spread in results between the different models (see Appendix B for individual model results). Only results for 2050 B1 are shown in Fig. 5, but the relative standard deviations for the other years and scenarios also have similar distributions. The robustness of the models is quite good for the aircraft perturbation case, with a relative standard deviation less than 20 % in most of the areas where the perturbation effect is strong. However, model differences in interhemispheric transport result in a larger relative standard deviation in the Southern Hemisphere (SH). The relative standard deviation for shipping demonstrates larger deviations between the models compared to the aircraft case, and is mainly in the range 30–40 %. One of the models (OsloCTM2) gives large impacts from shipping with a scaled maximum value of 2.5 DU, while another model (MOCAGE) has a corresponding value of only 0.9 DU. However, as model intercomparison is beyond the scope of this study, the reader is referred to e.g. Danilin et al. (1998) and Rogers et al. (2002) for thorough discussions of differences between CTMs.

4.1 Effects of aircraft emissions

Figure 6 shows the impact of aircraft emissions on ozone in the UTLS region for January and July along with the difference between the B1 and B1 ACARE scenarios (represented by the red lines). When focusing on the B1 scenario, the results indicate an increase in ozone impact from aircraft between 2000 (black dotted line) and 2025 (black dashed line), while the difference between 2025 and 2050 (black solid

line) depends on the season and on the latitude. Because of the strong net decrease in NO_x emissions from aircraft at northern mid- and high latitudes from 2025 to 2050 (Fig. 4), the resulting ozone effect is a decrease in zonal mean values north of 30° N during summer (Fig. 6, bottom right) when the photochemistry is more intense. This signal is to a large extent consistent between the models, but it depends strongly on the model whether or not there is an ozone decrease in the NH during winter. In the SH, the ozone impact from aircraft emissions is likely to increase in 2025 and further to 2050, if emissions evolve according to the B1 scenario. The zonal mean local maximum of 0.066 ppbv (or 1.3 ppbv scaled to 100 %) at about 25° S in 2050 B1 (July) is caused by a combination of increased emissions in the tropics (Fig. 4) and transport across the hemispheres.

The local maximum can also be seen in Fig. 7, which shows the zonal mean ozone impact for 2050 B1 (see Fig. B1 for individual model results), together with the average vertical profile of the NH impact on ozone for each year and scenario. The results show that the maximum absolute impact in the UTLS region is larger in July compared to January, because of the difference in the length of the day between both months. However, the maximum ozone impact relative to the reference simulation (BASE) in 2050 B1 is larger in January with a peak value of 0.21 % (or 4.2 % scaled) located in the middle to upper troposphere at 20–30° N. This peak in the tropics during winter arises because aircraft-induced NO_x and O_3 are transported from the northern mid-latitude UTLS to the low-latitude middle troposphere where the background levels of NO_x and O_3 are lower. For comparison, Grewe et al. (1999) calculated annual maximum relative ozone changes due to aircraft emissions of 7 % in a 2050 scenario, but the aircraft NO_x emissions used in their study were about twice as large as the 2050 B1 emissions that are used here (2.15 TgN yr^{-1} compared to 1.05 TgN yr^{-1}), and the surface NO_x emissions were 60 % larger (69.7 TgN yr^{-1} compared to 43.8 TgN yr^{-1}). The comparison is also influenced by several other factors such as the difference in year of meteorology used and potential model developments (e.g.
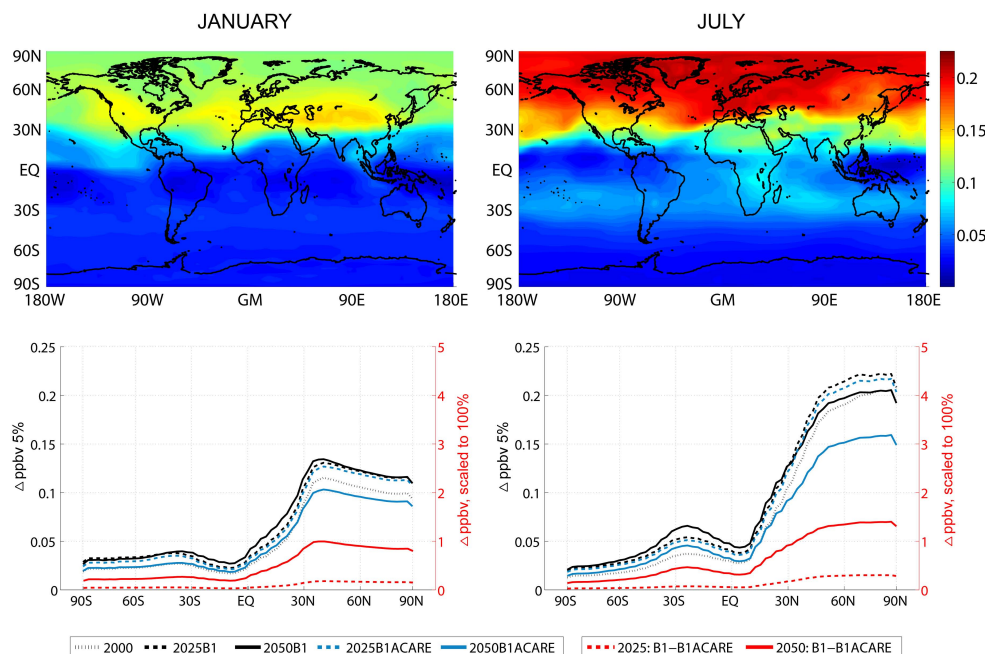
Fig. 6. Mean perturbations of ozone (Δppbv) in the upper troposphere (300–200 hPa) during January (left) and July (right) for the 2050 B1 scenario (top) and as zonal means for all scenarios (bottom). The color bar and the left y-axis show the unscaled impact of the 5 % perturbation of aircraft emissions (simulations BASE – AIR), while the red scales in the bottom figures are scaled up by a factor 20 from 5 % to 100 % and refer to all lines. The red lines show the difference between the B1 and B1ACARE scenarios and refer to the red axis only.
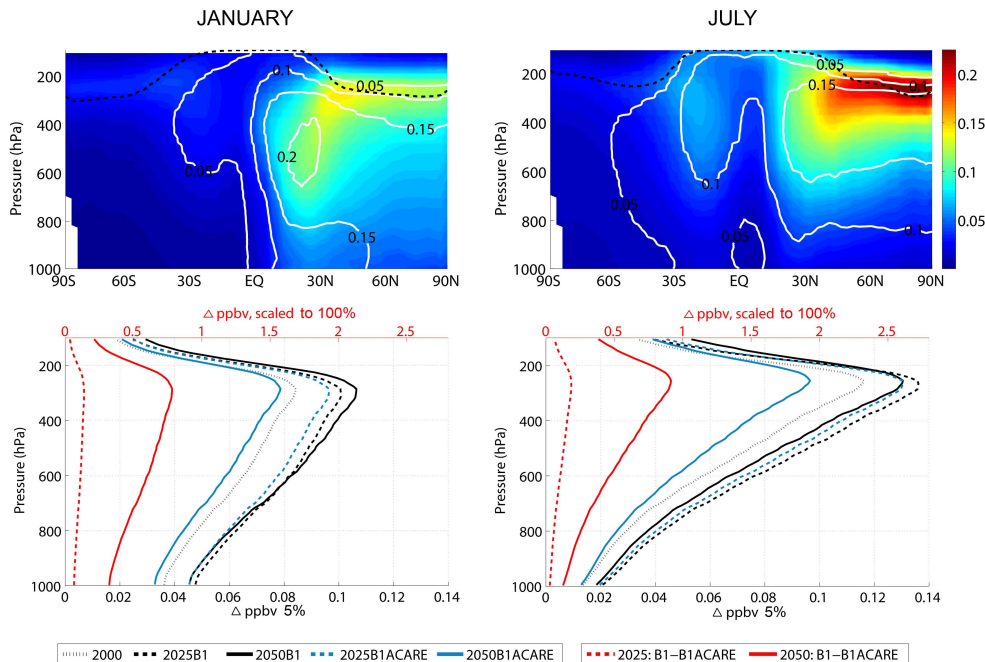
Fig. 7. Zonal mean perturbations of ozone (Δppbv) during January (left) and July (right) for the 2050 B1 scenario (top) and as Northern Hemisphere average for all years (bottom). In the top figures, solid contour lines show the change relative to the BASE simulation while the dashed line indicates the tropopause. The color bar and the bottom x-axis show the unscaled impact of the 5 % perturbation of aircraft emissions (simulations BASE – AIR), while the red scales in the bottom figures are scaled up by a factor 20 from 5 % to 100 % and refer to all lines. The red lines show the difference between the B1 and B1ACARE scenarios and refer to the red axis only.

Table 3. Global annual average of the change in O_3 molecules per NO_x molecule emitted from aviation and shipping, given as ensemble means and standard deviations.

	2000	2025B1	2050B1	2025B1ACARE	2050B1ACARE
AIR	2.05 (±0.51)	1.90 (±0.42)	2.16 (±0.52)	1.95 (±0.42)	2.31 (±0.59)
SHIP	0.509 (±0.185)	0.508 (±0.185)	0.535 (±0.194)	–	–

chemical reaction rates, deposition parameterizations, improved resolution) since the Grewe et al. (1999) study. Also worth noting is the fact that ozone perturbations in the lower troposphere are weaker during summer than in winter, presumably because the surface deposition to plants is faster and the photochemical lifetime of ozone is shorter (because increased water vapour gives more HO_x and thereby ozone loss) at lower altitudes during summer.

If emissions evolve according to the B1 ACARE mitigation option rather than the B1 scenario, Figs. 6 and 7 show that ozone will only be reduced by a small amount in 2025 (red dashed line), while in 2050 (red solid line) the mitigation option will have a substantial effect on reducing ozone levels. A direct comparison between B1 and B1 ACARE yields mean ozone differences poleward of 30° N in the UTLS of 0.18–0.30 ppbv and 0.94–1.40 ppbv during summers of 2025 and 2050, respectively (Fig. 6, red lines). Notably in the NH, the average ozone perturbation from aircraft in 2050 for B1 ACARE (blue solid line) is reduced to considerably lower values than the estimated impact in year 2000 (black dotted line) for altitudes below 200 hPa (Fig. 7). The fact that the mitigation option only has a minor effect in 2025 could be associated with the long lifetime of aircraft.

Hoor et al. (2009) found that the change in ozone burden per NO_x-emission was highest for aircraft when comparing with the road and ship transport sectors. In Table 3 we have presented the ozone enhancement efficiency in order to investigate how the sensitivity changes with different years and scenarios. Previous studies (e.g. Grooß et al., 1998; Grewe et al., 1999) have found that the non-linearity in the ozone production normally leads to a smaller positive ozone perturbation per aircraft emitted NO_x-molecule when the emissions are higher. This is also the case when we compare the ozone change per aircraft NO_x-emission in 2000 with 2025 (Table 3), when the emissions are expected to increase. However, when looking at the 2050 B1 scenario, all models show a higher ozone enhancement efficiency compared to year 2000, although the aircraft NO_x emissions also are higher. This unexpected effect can be explained by the change in the location of the emissions. In 2050, the aircraft NO_x emissions are shifted further south compared to year 2025 (Fig. 4), and will then take place in more pristine regions where the background NO_x levels are lower. Additionally, Hoor et al. (2009) emphasized the role of road traffic for the chemical state of the UTLS, and as NO_x emissions

from this transport sector are assumed to decrease rapidly in the future, the NO_x background levels at cruise altitude are affected. Not surprisingly, the highest ozone enhancement efficiency is found in 2050 B1 ACARE, which is the scenario with the lowest aircraft emissions. For this case, the models estimate that the ozone abundance increases by 2.31 molecules for every NO_x molecule emitted from aircraft.

4.2 Effects of ship emissions

Figures 8 and 9 show the effects of shipping emissions on atmospheric ozone in January and July for different years and scenarios (see Fig. B2 for individual model results). Even if emissions evolve according to the optimistic B1 scenario, model results show that the shipping sector will increase its effect on ozone in the future. Focusing on the estimated ozone impact in the lower troposphere in 2050 B1 (Fig. 8), the largest effect from shipping can be found in the North Atlantic Ocean with ozone values of about 0.2 ppbv (or 4 ppbv scaled) during summer when the photochemical activity reaches a maximum. Notably, the impact in the Arctic region is expected to increase in the future due to the expected introduction of new ship tracks associated with melting of the polar ice cap. This area is especially sensitive to emission perturbations because of the low background NO_x levels which lead to higher ozone enhancement efficiencies. Consequently, the maximum relative effects in July are found in this region, showing zonal mean impacts exceeding 0.6 % (or 12 % scaled) near the surface (Fig. 9).

Interestingly, Fig. 8 shows that the ozone impact from shipping at northern mid- and high latitudes will increase from 2025 (dashed line) to 2050 (solid line), especially during winter, although the emissions in these regions are expected to decrease (Fig. 4). Except for transport from lower latitudes, where the emissions increase, this feature can be explained by lower ambient levels of NO_x which act to increase the change in ozone burden per NO_x emitted from ships. The increase in ozone enhancement efficiency can also be seen in Table 3, where global annual average values are given. In the future B1 scenario, large reductions in anthropogenic non-traffic and road emissions of NO_x are assumed over the Eastern US and Europe. This significantly increases the ozone enhancement efficiency from shipping, as transport from these polluted continental areas normally leads to higher levels of NO_x over the Atlantic Ocean and the North Sea.
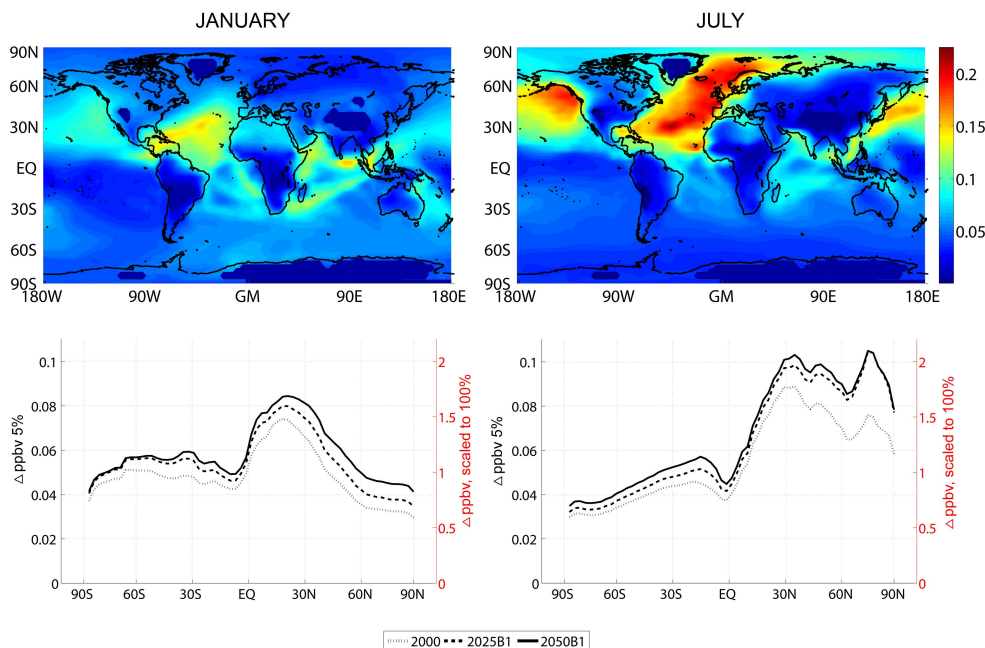
Fig. 8. Mean perturbations of ozone (Δppbv) in the lower troposphere (>800 hPa) during January (left) and July (right) for the 2050 B1 scenario (top) and as zonal means for all years (bottom). The color bar and the left y-axis show the impact caused by a 5 % perturbation of ship emissions (simulations BASE – SHIP), while the red scales in the bottom figures are scaled up by a factor 20 from 5 % to 100 %.
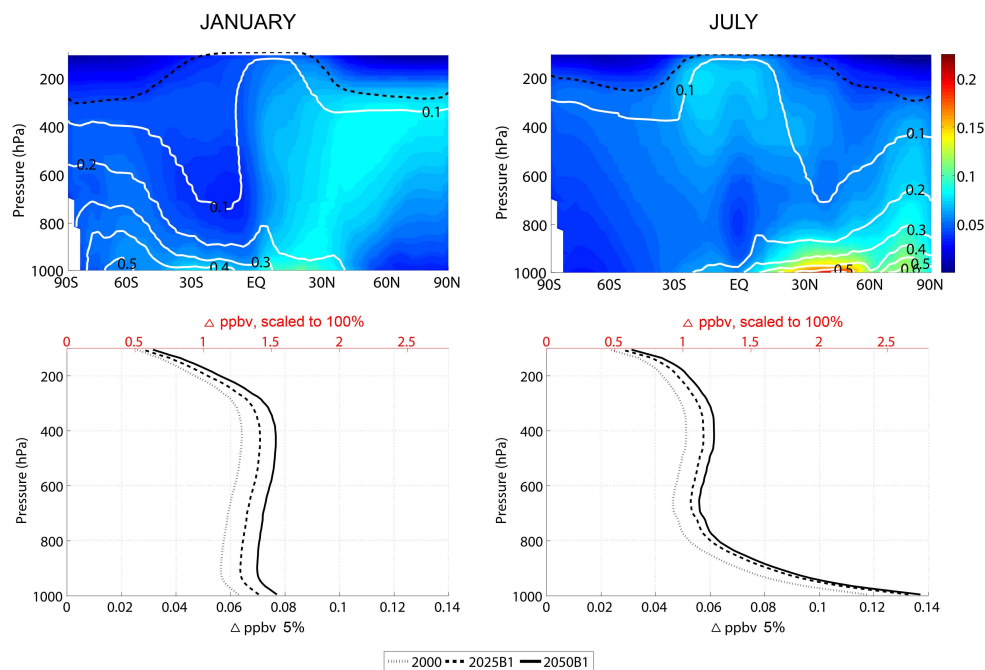
Fig. 9. Zonal mean perturbations of ozone (Δppbv) during January (left) and July (right) for the 2050 B1 scenario (top) and as Northern Hemisphere average for all years (bottom). In the top figures, solid contour lines show the change relative to the BASE simulation while the dashed line indicates the tropopause. The color bar and the bottom x-axis show the impact caused by a 5 % perturbation of ship emissions (simulations BASE – SHIP), while the red scales in the bottom figures are scaled up by a factor 20 from 5 % to 100 %.
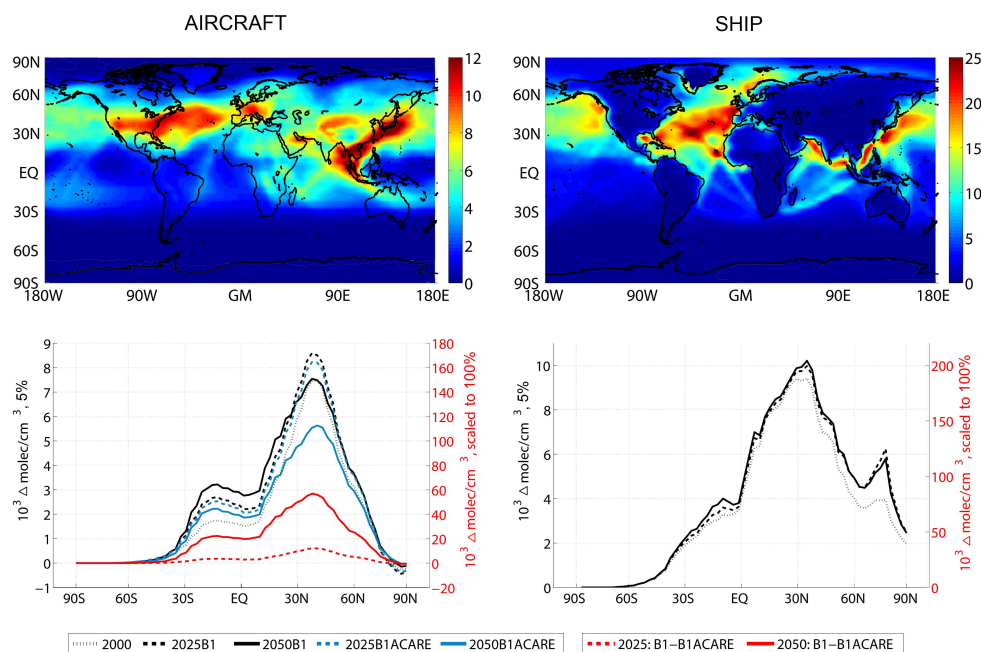
Fig. 10. Mean perturbations of OH (10^3 Δmolec cm^{-3}) in July in the upper troposphere (300–200 hPa) due to a 5 % perturbation of aircraft emissions (left), and in the lower troposphere (>800 hPa) due to a 5 % perturbation of ship emissions (right). The top row figures show results from the 2050 B1 scenario, and the bottom row figures show zonal means for all years and scenarios. The colorbars and the left y-axis show the unscaled impact of the 5 % perturbation of the emissions, while the red scales in the bottom figures are scaled up by a factor 20 from 5 % to 100 % and refer to all lines. The red lines show the difference between the B1 and B1ACARE scenarios and refer to the red axis only. Note that different scales are used for AIR and SHIP.

5 OH

5.1 Global OH

Changes in the concentration and distribution of the hydroxyl radical (OH) are important for air pollution and the self-cleaning capacity of the atmosphere (Lelieveld et al., 2002) as OH is the main oxidant in the troposphere. Validation of modelled OH is difficult, however, particularly because of its short lifetime (less than one second) which makes it almost impossible to measure directly. In a recent study by Montzka et al. (2011), indirect measurements of the interannual variability of global OH are consistent with past model studies (Dentener et al., 2003; Dalsøren and Isaksen, 2006; Lelieveld et al., 2006; Duncan and Logan, 2008), and this suggest that larger confidence should be given to models than previously assumed (Isaksen and Dalsøren, 2011).

The impact of aircraft and shipping emissions on tropospheric OH is shown in Figs. 10 and 11 for July, when the effect is largest due to enhanced photochemistry in the NH. For aircraft emissions, there is an indication of a future increase in the impact on tropospheric OH. Figure 10 shows that enhanced OH levels in the UTLS are expected at all latitudes in 2025 (black and blue dashed lines), with an exception near the Arctic region where increased aircraft emissions seem to cause a slight decrease in OH levels. However, when comparing the impacts between 2025 and 2050, the OH response depends strongly on both scenario and latitude. In 2050 (black and blue solid lines), a decrease is seen between approximately 30 and 60° N, associated with a strong decrease in aircraft NO$_x$ emissions (Fig. 4), while a zonal mean increase is expected elsewhere, in particular near the equator where aircraft NO$_x$ emissions are assumed to increase. In 2025 B1, the zonal mean average in the UTLS region for July peaks at 40° N with a value of 8.6×10^3 molecules cm^{-3} (unscaled). When averaging the aircraft-induced OH vertical profile over the entire NH, 2025 B1 and 2050 B1 both show a maximum of 5.4×10^3 molecules cm^{-3} (unscaled) near 250 hPa (Fig. 11).

The largest effects from aircraft emissions during northern summer in the future (July 2050; B1) can be found east and southeast of Asia, but also with significant impacts close to the North Atlantic flight corridor (Fig. 10, top left). The zonal mean OH impact peaks above 300 hPa, and this is also the region of maximum relative impact with a value of 0.6 % (or 12 % scaled) (Fig. 11, top left). In the SH, the absolute values are lower, but due to low background levels the relative impact is fairly high with a value of almost 0.5 % (or 10 % scaled).

As was the case with ozone, the technological improvements that are assumed in the B1 ACARE mitigation scenario have significant effects on OH. If the ACARE targets
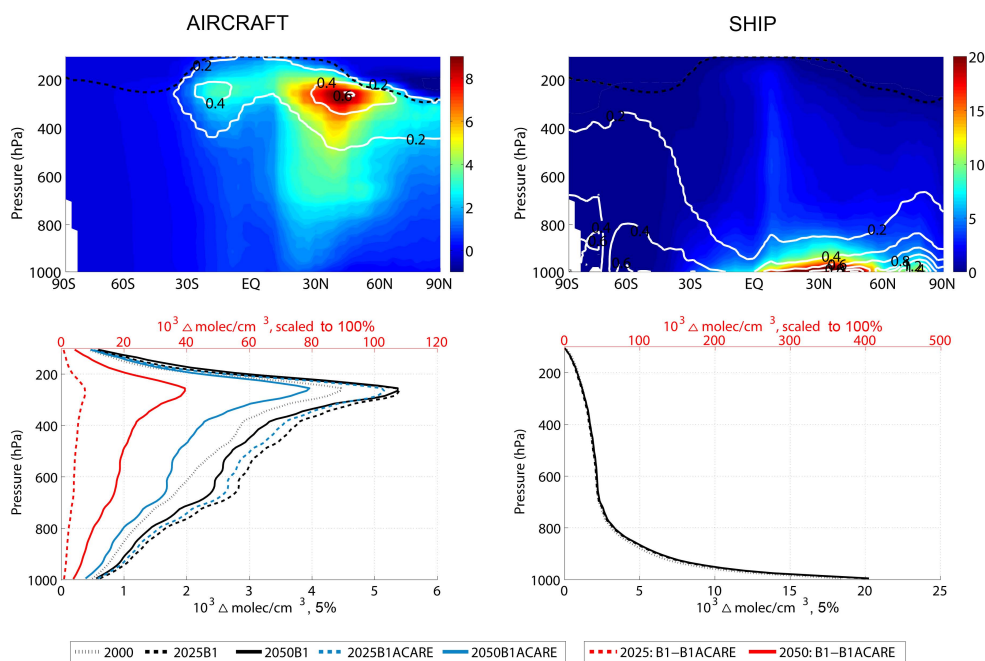
Fig. 11. Zonal mean perturbations of OH (10^3 Δmolec cm^{-3}) in July due to a 5 % perturbation of aircraft emissions (left) and ship emissions (right), for the 2050 B1 scenario (top) and the average Northern Hemisphere vertical profile for all years and scenarios (bottom). In the top figures, solid contour lines show the change relative to the BASE simulation while the dashed line indicates the tropopause. The colorbar and the bottom x-axis show the unscaled impact of the 5 % perturbation of the emissions, while the red scales in the bottom figures are scaled up by a factor 20 from 5 % to 100 % and refer to all lines. The red lines show the difference between the B1 and B1ACARE scenarios and refer to the red axis only. Note that different scales are used for AIR and SHIP.

will be met in 2050, the northern summer OH levels in the UTLS region (red solid line) could be reduced by up to 5.7×10^4 molecules cm^{-3} (Fig. 10, bottom left). The reductions are substantial also in the NH as a whole, showing average differences between B1 and B1 ACARE of 3.9×10^4 molecules cm^{-3} near 250 hPa (Fig. 11, bottom left), and with significant effects also in the middle troposphere. In the near future (2025), the gain of fulfilling the ACARE targets is much lower, but still the maximum difference between B1 and B1 ACARE is 7.6×10^3 molecules cm^{-3} (red dashed line).

Hoor et al. (2009) emphasized the large impact of ship emissions on the boundary layer OH levels, and concluded that the effect of ship emissions is more important for the global OH budget than road and aircraft emissions. Figure 10 shows that the impact from ship emissions on OH in the boundary layer is expected to increase in the future if emissions evolve according to the B1 scenario. Between 2025 and 2050, OH will continue to increase at all latitudes except north of 60° N where a small reduction in ship NO$_x$ emissions is expected.

Focusing on northern summer in the future (July 2050; B1), the largest impact from ship emissions can be found in the North Atlantic Ocean with maximum values reaching 3.0×10^4 molecules cm^{-3} (unscaled) (Fig. 10, top right).

As discussed in Sect. 4.2, ozone production in this area is largely sensitive to an increase in NO$_x$ emissions, and because of high humidity and strong incoming solar radiation, additional OH is produced when O(^{1}D) reacts with H$_2$O. Additionally, the background levels of CO and NMHCs, which act to deplete OH, are relatively low in these pristine regions. In the zonal mean, maximum absolute values are found near the surface at 45° N (Fig. 11, top right), while the relative impact reaches a maximum of about 1.5 % (or 30 % scaled) near 75° N. The reason is the low background values of OH, as shipping is a dominant source of air pollutants at these high latitudes, and because the production of additional OH caused by ship emissions is more effective in the summer month of July.

5.2 Methane lifetime

Emissions from the aircraft and shipping sectors greatly affect the OH concentration, and this leads to changes in the methane lifetime. Methane lifetimes due to reaction with OH have been calculated for each model and for each year and scenario. As in Hoor et al. (2009), monthly mean 3-D fields of methane and OH were used, and the resulting lifetime changes were then scaled from a 5 % perturbation in emissions to a 100 % perturbation (to get a stronger signal in the RF calculations) by multiplying with a factor of 20

Table 4. Relative changes (%) in methane lifetimes (integrated up to 50 hPa) due to a 5 % decrease in traffic emissions. Values are given relative to the BASE case, and are scaled to 100 % by multiplying with 20. Both the mean of the six models and the standard deviations (indicating the spread of the models) are given. Note that this table does not include the feedback effect of methane changes on its own lifetime.

	AIR	SHIP
2000	1.30 ($\pm$0.30)	3.68 ($\pm$0.47)
2025B1	1.69 ($\pm$0.35)	3.73 ($\pm$0.40)
2050B1	1.68 ($\pm$0.38)	3.92 ($\pm$0.48)
2025B1ACARE	1.59 ($\pm$0.34)	–
2050B1ACARE	1.17 ($\pm$0.28)	–

(Grewe et al., 2010). The resulting model mean and standard deviation of the methane lifetime changes are given in Table 4 (see Tables B1–B2 for individual model results), while the model mean of the methane lifetime is 8.0 ($\pm$1.0) yr in the 2050 B1 BASE simulation and 8.3 ($\pm$1.0) yr in the 2000 BASE simulation. The rather low relative standard deviation of 12 % is similar for the BASE simulations of the other scenarios, and indicates that the ensemble mean of the models is relatively robust when calculating methane lifetimes.

As discussed in Sect. 5.1, SHIP exhibits the largest impact on OH levels and consequently the largest impact on methane lifetime. The model ensemble predicts that the shipping sector contributed to a methane lifetime reduction of 3.68 % in year 2000, and that this number will increase to 3.92 % in 2050, if emissions evolve according to the B1 scenario (Table 4). Eyring et al. (2007) calculated methane lifetime changes from shipping in 2030, and their estimates range from 1.14 % to 1.81 % for a low and high emission scenario, respectively. Their result is much lower than both 2025 B1 and 2050 B1 from this study, and that was also the case for the year 2000 results discussed in Hoor et al. (2009). According to Hoor et al. (2009), part of the differences could be attributed to the very different distribution of ship emissions. The same reasoning applies here as the future ship emissions in Eyring et al. (2007) are more concentrated along the major shipping routes in contrast to the QUANTIFY future ship emissions, which are spread out over larger areas.

The methane lifetime changes for SHIP do not follow the trend in ship NO_x emissions, which increased a lot more between 2000 and 2025 B1 than between 2025 B1 and 2050 B1 (Fig. 1). The reason is the assumption of large reductions in land based NO_x emissions, particularly from road traffic, in Europe and the US between 2025 B1 and 2050 B1 (not shown). This effect exceeds the impact of increased ship emissions, as a decrease in background NO_x levels leads to a more efficient OH production from shipping.

The future methane lifetime changes for AIR are to a certain degree in accordance with the evolution of the aircraft

B1 emissions; an increased impact in 2025 followed by stabilization in 2050 (Table 4). The model ensemble predicts a much lower impact of aircraft on methane lifetimes for the B1 ACARE scenario, especially in 2050 when the relative methane lifetime change is lower than the year 2000 value.

6 Radiative forcings

Radiative forcings have been calculated using the same method as in Myhre et al. (2011). The Oslo radiative transfer model (Myhre et al., 2000) was used to calculate ozone radiative forcings based on monthly mean ozone fields from each model simulation. In order to obtain a robust signal the fully scaled perturbations have been used in the RF calculations, i.e. the ozone change resulting from the 5 % perturbation has been multiplied by 20 (Hoor et al., 2009; Grewe et al., 2010). According to Myhre et al. (2011), the non-linearities arising from the perturbation magnitude are of little importance compared to the inter-model differences in the RF.

Figure 12 shows the yearly averaged ozone RF for the 2050 B1 scenario as means of all models and with absolute standard deviations. The aircraft sector has a larger impact than ship emissions in the NH and the changes in RF are relatively homogeneous throughout different latitude zones. The impacts are large throughout the NH and have maximum values reaching 76 mW m^{-2} near 30° N. In the SH the ozone RF from aircraft is low, except in the region 0–30° S. This latitude band also shows a large spread of the models with standard deviations up to 21 mW m^{-2}, indicating possible model uncertainties related to convection and transport between the hemispheres. For SHIP, the ozone RF is stronger in the SH compared to AIR, but the RF in the NH is much weaker. Maximum impact from SHIP takes place between 30° N and 30° S, and peaks at 50 mW m^{-2}.

Global average ozone RF for all scenarios is given in Table 5 (see Tables B3–B4 for individual model results). For the B1 scenario there is a small increase in the ozone RF from AIR between 2025 and 2050, although the NO_x emissions from aircraft are assumed to decrease slightly during this time span. As explained in Sect. 4.1, this is probably caused by the latitudinal shift in the location of the aircraft emissions leading to higher ozone enhancement efficiencies in 2050. For comparison, Myhre et al. (2011) calculated a five model average of 17 mW m^{-2} for AIR in year 2000. The increase to 25.7 mW m^{-2} for 2025 B1 (Table 5) is consistent with the aircraft NO_x emissions, which also are assumed to increase (Fig. 1). For the 2050 B1 scenario, Skeie et al. (2009) estimated ozone RF from AIR to be 38 mW m^{-2} using a simple climate model. The relatively large difference to our study can be partly explained by a lower normalized radiative forcing in this study (36.3 compared to 42.9 mW m^{-2}DU^{-1}), and partly by lower ozone enhancement efficiencies (2.16 compared to 2.69 ozone molecules enhanced per NO_x molecule emitted from AIR). In Lee et al. (2009), a scaling approach

Table 5. Radiative forcings (mW m^{-2}) from changes in ozone, methane (including stratospheric water vapour), and methane-induced ozone for different transport sectors and years/scenarios given as ensemble means and standard deviations. Note that the history of emissions has been taken into account, and that the fully scaled perturbations were used.

| | AIRCRAFT | | | | SHIPPING | | | |
	O_3	CH_4	$O_{3(CH4)}$	total	O_3	CH_4	$O_{3(CH4)}$	total
2025B1	25.7 (±8.3)	−16.0 (±3.4)	−5.9 (±1.2)	3.8 (±6.1)	23.6 (±8.4)	−37.8 (±4.1)	−13.8 (±1.5)	−28.0 (±5.1)
2050B1	26.2 (±9.0)	−17.8 (±4.0)	−6.5 (±1.5)	1.9 (±6.4)	25.2 (±9.6)	−41.0 (±5.0)	−15.0 (±1.8)	−30.8 (±4.8)
2025B1ACARE	24.1 (±7.7)	−15.5 (±3.3)	−5.7 (±1.2)	2.9 (±5.8)	–	–	–	–
2050B1ACARE	18.9 (±6.8)	−14.3 (±3.4)	−5.2 (±1.2)	−0.6 (±4.6)	–	–	–	–
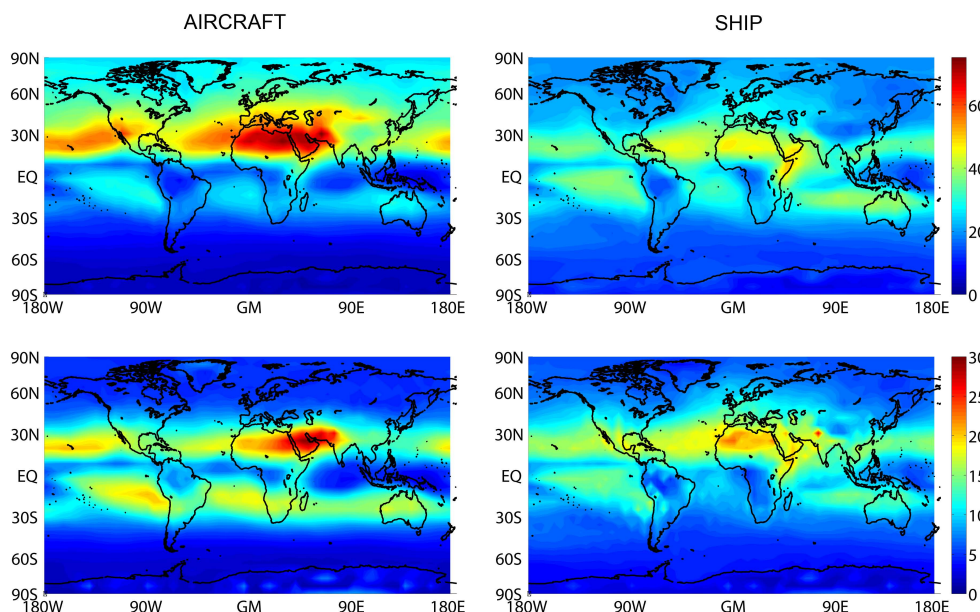
Fig. 12. Radiative forcing (mW m^{-2}) from short-term O_3 due to emissions from aircraft (left) and shipping (right), shown as ensemble mean for the 2050 B1 scenario (top) along with the absolute standard deviation (bottom). Note that the fully scaled perturbations were used to calculate the forcings.

was used to estimate the aviation RF of ozone in 2050 to be in the range 59.4–109.8 mW m^{-2}, depending on the scenario. Their estimates are much higher than in this study, but this is expected because even their lowest emission scenario (SRES B2 with technology 2, see IPCC, 1999) had larger aircraft NO$_x$ emissions than the 2050 B1 scenario used here. The effect of the B1 ACARE mitigation strategy is evident already in 2025, with a 1.6 mW m^{-2} lower ozone RF than in the B1 scenario (Table 5). However, in 2050 the corresponding number has increased to 7.3 mW m^{-2}, showing the large potential impact of technological improvements in the aircraft sector.

The ozone RF from SHIP is calculated to increase between 2025 and 2050, this time due to a combination of the slight increase in ozone precursor emissions for this transport sector, and the stronger ozone enhancement efficiency in 2050 (see Sect. 4.2). Despite the assumed increase in ship emissions between 2000 and 2025 B1, Myhre et al. (2011)

have a larger estimate for 2000 (24 mW m^{-2}) than our results for 2025 B1. The reason is that the MOCAGE model is included in our study, and this model is at the lower end of the spectrum when calculating ozone RF from SHIP (Table B4). Again, Eyring et al. (2007) calculated lower impacts than in this study, with ozone RF from shipping ranging from 7.9 to 13.6 mW m^{-2} in 2030. On the other hand, Skeie et al. (2009) estimated a larger impact from shipping with short-lived ozone RF at 36 mW m^{-2} for the 2050 B1 scenario, also this time due to lower ozone enhancement efficiencies in this study (0.535 compared to 0.859 ozone molecules enhanced per NO$_x$ molecule emitted from SHIP).

Emissions of NO$_x$ from aircraft and shipping sectors normally lead to an increase in OH concentrations, resulting in a reduction of methane lifetime. The forcing due to the changes in methane is given in the second column in Table 5, and has been calculated mainly using the method described by Berntsen et al. (2005). For each year and scenario, the

changes in methane lifetime were multiplied by the estimated methane concentrations reported in IPCC (2001). Further, to account for the impact of methane changes on its own lifetime, a feedback factor of 1.4 was used (IPCC, 2001). The linearized methane specific forcing of $0.35 \, \text{mW} \, \text{m}^{-2} \, \text{ppbv}^{-1}$ was then applied, assuming a background methane mixing ratio of 1909 ppbv and 1881 ppbv for 2025 B1 and 2050 B1, respectively. In Table 5, the CH_4 RF term includes the impact of methane changes on stratospheric water vapour (SWV), and the RF of SWV is assumed to be 0.15 times that of the methane RF (Myhre et al., 2007).

RF from changes in methane-induced ozone is calculated assuming that a 10 % increase in methane leads to a 0.64 DU increase in ozone (IPCC, 2001), and that this ozone has a specific forcing of $42 \, \text{mW} \, \text{m}^{-2} \, \text{DU}^{-1}$ (IPCC, 2001). As explained in Myhre et al. (2011), the chemical model calculations are one year simulations only, hence the methane concentration may not be in steady state with the change in OH during that year, but depends on the time-history of the emissions. In order to correct for this transient response, factors have been applied based on the method described in Grewe and Stenke (2008). The factors for 2025 are 0.88, 0.91 and 0.94 for AIR B1, AIR B1ACARE and SHIP B1, respectively. Corresponding factors for 2050 are 1.00, 1.15 and 0.99. Note that the factor for 2050 B1 ACARE is larger than 1 because the aircraft emissions are assumed to decrease in the preceding years for this scenario.

The sum of the three RF components in Table 5 shows a negative RF from SHIP, and this is consistent with what has been found in previous studies (Fuglestvedt et al., 2008; Skeie et al., 2009; Myhre et al., 2011). For AIR, however, the total RF is slightly positive in three out of four cases. Interestingly, a slightly negative RF is predicted for the 2050 B1 ACARE scenario. It is important to note that the net effect for AIR is the sum of a fairly large positive number (O_3 RF) and two smaller negative numbers (CH_4 plus CH_4-induced O_3 RF), each associated with uncertainties. The subtle difference between these effects results in a small net value, and considering the uncertainties it is difficult to say for sure whether or not the net effect is positive or negative. However, the general tendency of an increasing importance of methane RF relative to the ozone RF for future air traffic emissions is consistent for both B1 scenarios. It reflects the decreasing rate of ozone RF increase, whereas the CH_4 RF decreases are effective with a time-lag associated with the methane lifetime. For the B1 scenario, a reduction of $1.9 \, \text{mW} \, \text{m}^{-2}$ is predicted between 2025 and 2050, and for B1 ACARE the reduction is $3.5 \, \text{mW} \, \text{m}^{-2}$. Compared to Myhre et al. (2011), our estimates of total RF may seem low considering that the aircraft NO_x emissions are higher for the B1 scenario in 2025 and 2050 than they were in 2000. The reason is related to the factors used to correct for the time-history of the emissions, which has to be kept in mind when interpreting RF from methane plus induced ozone changes. The aircraft NO_x emissions increased rapidly prior to year 2000, while the increase levelled off towards 2025, and further turned to a reduction towards 2050 in the B1 and B1 ACARE scenarios. As a consequence, the cooling effect caused by changes in methane and methane-induced ozone RF may compensate the warming from short-term ozone RF (which is unaffected by the time-history of emissions), if emissions evolve according to the optimistic B1 or B1 ACARE scenarios.

7 Conclusions

Six atmospheric chemistry models have been applied in order to investigate how emissions from the non-land based traffic sectors (AIR and SHIP) impact the distributions of ozone and OH according to the B1 and B1 ACARE emission scenarios. Although the B1 scenario is considered optimistic, model results show that the impacts of both AIR and SHIP emissions on ozone and OH will increase in the future (2025 and 2050) compared to recent time (2000). We used the perturbation approach to calculate both, the contributions of the individual sectors to ozone and OH, and their changes over time, knowing that this methodology has principle limitations in the calculation of contributions (Grewe et al., 2010). The choice of -5% emission perturbations guarantees a consistent calculation of the atmospheric sensitivity with respect to aircraft and ship emissions (Hoor et al., 2009). Our contribution calculation highlights the large impact of ship emissions on the chemistry in the lower troposphere, and indicates that ship-induced ozone could exceed 4 ppbv over the North Atlantic Ocean during future summer (July 2050; B1). At the same time, aircraft emissions dominate in the UTLS region with a maximum zonal mean ozone impact that could reach 5 ppbv polewards of $30° \text{N}$.

Model simulations with the B1 ACARE mitigation scenario for aviation show modest reductions in ozone levels in 2025, while substantial reductions can be expected in 2050. Zonal means of the UTLS region at northern mid- and high latitudes show that B1 ACARE yields 0.9–1.4 ppbv lower ozone values than the already optimistic B1 scenario during future summer (July 2050), and this is even lower than for recent time (2000). However, all of our future simulations predict an increase in aircraft-induced ozone in the SH compared to year 2000, and this is mainly a response to the assumed increase in aircraft NO_x emissions in this region. Additionally, the shift in emission location between 2025 and 2050, from the already polluted mid- and high northern latitudes to the more pristine regions in the south, leads to an increase in the ozone enhancement efficiency with an increase in the ozone concentration of 2.31 molecules per emitted aircraft NO_x molecule for the 2050 B1 ACARE scenario.

Emissions from SHIP have important effects on the OH concentrations, particularly in the marine boundary layer, and this impact will become increasingly important in the future. As a consequence, the models estimate a relative methane lifetime reduction of 3.9 % (scaled) due to SHIP in
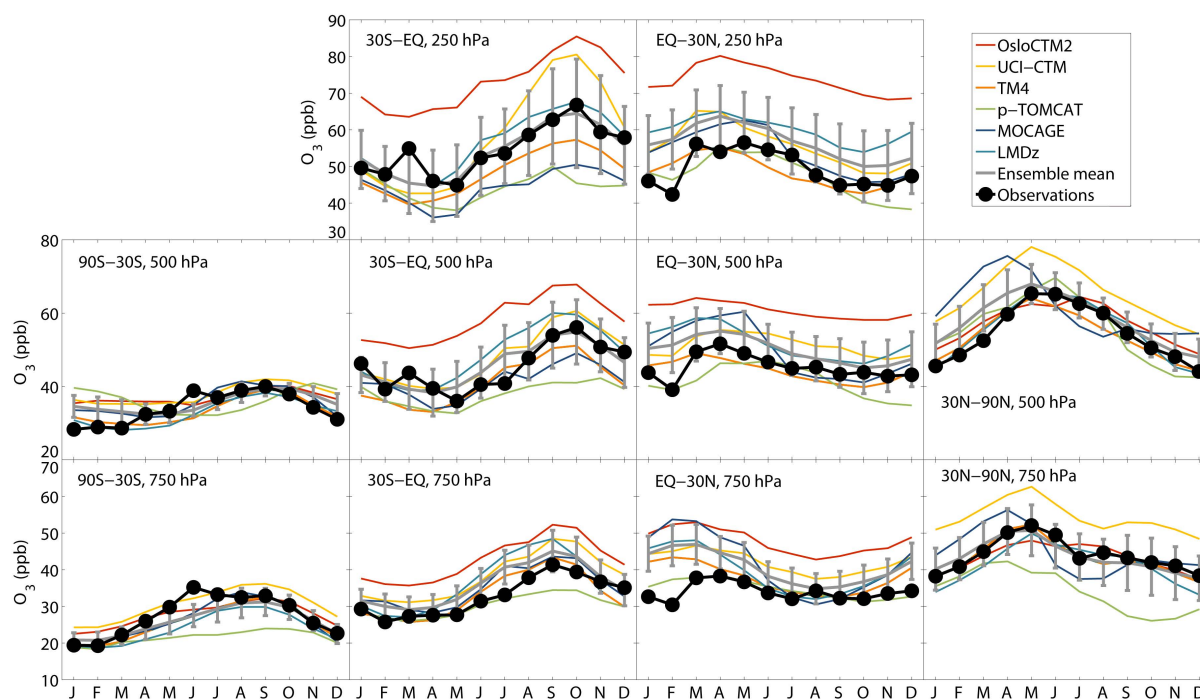
Fig. A1. Comparison of the monthly mean ozone observations (black line with dots) from Logan (1999) with the model ensemble mean and standard deviation (grey line with error bars), and the individual model results (see legend for color codes) at different latitude bands (from left to right: 90° S–30° S, 30° S–EQ, EQ–30° N, 30° N–90° N) and different pressure levels (from top to bottom: 250 hPa, 500 hPa, 750 hPa) for the 2003 model simulations. For comparison, the figure has been made similar to Fig. 2 in the multi-model study by Stevenson et al. (2006).

2050 B1. The corresponding value for AIR is 1.7 %, but if the ACARE targets will be achieved, this number is reduced to 1.2 %.

The large impact of SHIP on OH is reflected in the radiative forcing calculations. When considering RF from changes in short-term ozone, methane (including stratospheric water vapour), and methane-induced ozone, our results suggest that SHIP will have a net cooling effect in 2025 and 2050 of -28.0 (±5.1) and -30.8 (±4.8) mW m^{-2}, respectively, for the B1 scenario. The uncertainties relative to net RF are larger for AIR, but positive RF from short-term ozone normally dominates. The resulting RF for AIR in the B1 scenario is 3.8 (±6.1) and 1.9 (±6.3) mW m^{-2} in 2025 and 2050, respectively. Interestingly, a small cooling effect of -0.6 (±4.6) mW m^{-2} is estimated for 2050 B1 ACARE, but it is important to note that the time-history of emissions has been taken into account, and this leads to a dominance of RF caused by changes in methane and methane-induced ozone, as the larger aviation emissions prior to 2050 have no impact on the 2050 short-term ozone RF (due to shorter lifetime of ozone compared to methane). In order to obtain knowledge of the total impact from AIR and SHIP on future climate, the RF from CO$_2$, contrails (including contrail-cirrus) and aerosols must be considered in addition to the RF from ozone and methane presented here.

To summarize, emissions from the two transport sectors aviation and shipping will have an increased impact on atmospheric ozone and OH in the future, even if emissions evolve according to the optimistic B1 scenario. However, the aviation impact through ozone formation can be reduced significantly by initiating the ACARE mitigation option, which is purely based on technological improvements. The long operating time of aircraft suggests that mitigation measures for this traffic sector should be considered at an early stage.

Appendix A

Comparison with ozone observations

Results from the BASE simulation of each model have been compared to ozonesonde observations from Logan (1999) and are shown in Fig. A1. In general, the model results agree relatively well with the observations both regarding magnitude and annual cycle. However, a few exceptions can be found, particularly in the tropics where the OsloCTM2 model is biased high. This bias is well-known from previous studies and recent model development has shown that the inclusion of an HNO$_3$ forming branch of the HO$_2$ + NO reaction reduced tropical tropospheric O$_3$ modelled by OsloCTM2 significantly and improved the agreement with ozonesonde

Table B1. Relative changes (%) in methane lifetimes (integrated up to 50 hPa) due to a 5 % decrease in aircraft emissions. Values are given relative to the BASE case, and are scaled to 100 % by multiplying with 20. Note that this table does not include the feedback effect of methane changes on its own lifetime.

	TM4	p-TOMCAT	OsloCTM2	LMDz-INCA	UCI CTM	MOCAGE
2000	1.27	1.61	0.85	1.07	1.60	1.41
2025B1	1.82	2.03	1.11	1.40	1.93	1.84
2050B1	1.77	2.04	1.09	1.37	2.04	1.78
2025B1ACARE	1.71	1.93	1.05	1.32	1.82	1.73
2050B1ACARE	1.22	1.47	0.75	0.94	1.43	1.23

**Table B2.** Same as Table B1, but due to a 5 % decrease in ship emissions.

	TM4	p-TOMCAT	OsloCTM2	LMDz-INCA	UCI CTM	MOCAGE
2000	4.17	3.44	3.77	3.20	4.28	3.24
2025B1	4.20	3.49	3.96	3.36	4.08	3.27
2050B1	4.38	3.56	4.14	3.51	4.52	3.43

Table B3. Radiative forcings ($mW\,m^{-2}$) from changes in ozone, methane (including stratospheric water vapour), and methane-induced ozone for different years/scenarios, due to emissions from aircraft. Note that the history of emissions has been taken into account, and that the fully scaled perturbations were used.
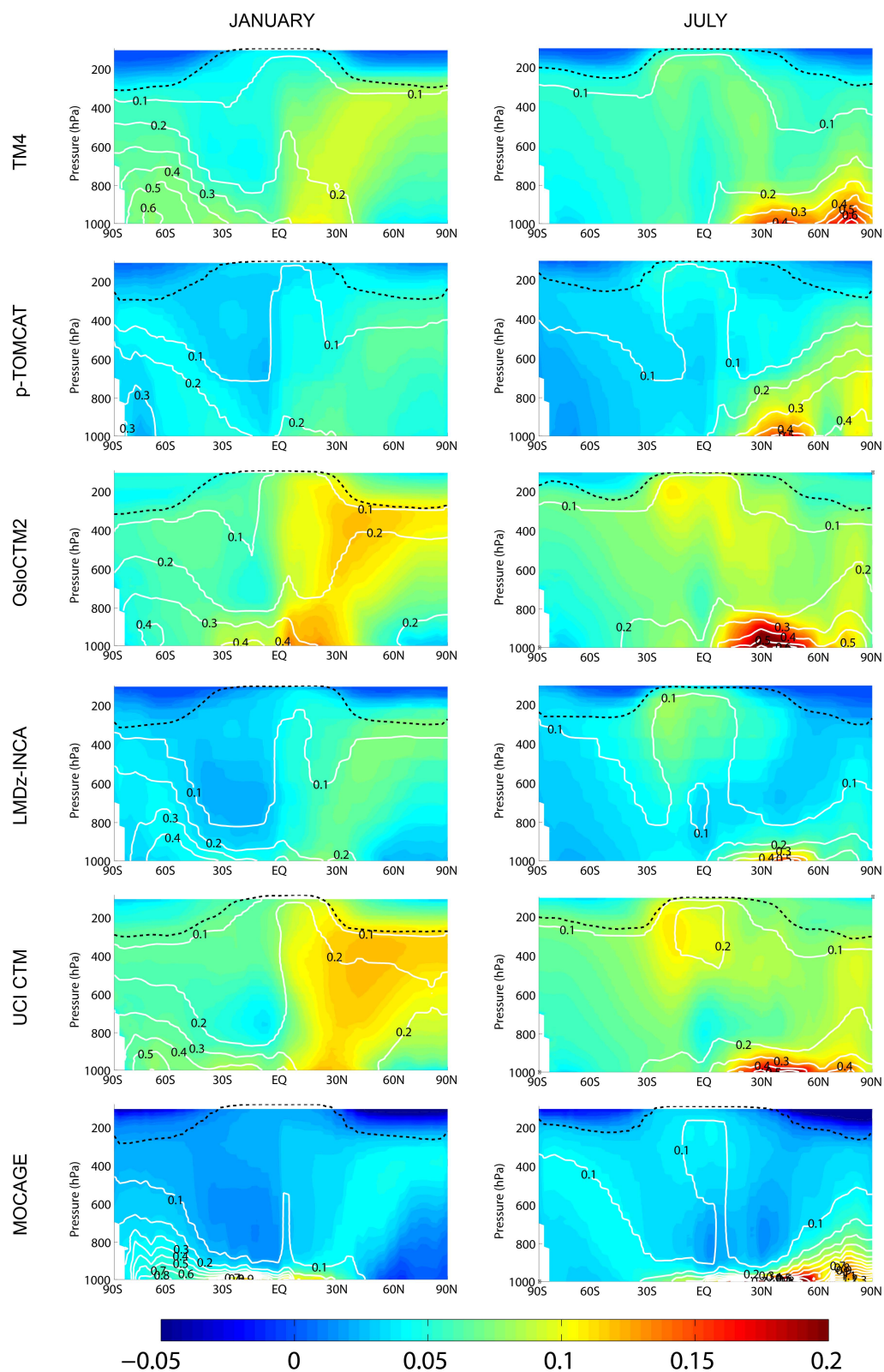
	TM4				p-TOMCAT				OsloCTM2			
	O_3	CH_4	$O_{3(CH_4)}$	total	O_3	CH_4	$O_{3(CH_4)}$	total	O_3	CH_4	$O_{3(CH_4)}$	total
2025B1	19.8	−17.3	−6.3	−3.8	40.1	−19.3	−7.0	13.8	20.6	−10.6	−3.9	6.2
2050B1	21.1	−18.8	−6.9	−4.5	42.7	−21.6	−7.9	13.2	20.4	−11.5	−4.2	4.7
2025B1ACARE	18.7	−16.6	−6.1	−4.0	38.2	−18.8	−6.9	12.6	20.3	−10.2	−3.7	6.4
2050B1ACARE	15.1	−14.8	−5.4	−5.2	31.4	−17.8	−6.5	7.1	14.6	−9.1	−3.3	2.1

	LMDz-INCA				UCI CTM				MOCAGE			
	O_3	CH_4	$O_{3(CH_4)}$	total	O_3	CH_4	$O_{3(CH_4)}$	total	O_3	CH_4	$O_{3(CH_4)}$	total
2025B1	18.0	−13.3	−4.9	−0.2	26.6	−18.3	−6.7	1.6	29.2	−17.5	−6.4	5.4
2050B1	18.0	−14.5	−5.3	−1.8	28.1	−21.6	−7.9	−1.4	27.2	−18.9	−6.9	1.4
2025B1ACARE	16.9	−12.8	−4.7	−0.6	25.1	−17.7	−6.5	0.9	25.5	−16.8	−6.1	2.5
2050B1ACARE	12.5	−11.4	−4.2	−3.1	19.9	−17.4	−6.4	−3.8	20.1	−14.9	−5.5	−0.3

measurements in the tropics (Søvde et al., 2011). Furthermore, modelling of tropospheric ozone and its precursors is particularly difficult in the tropics due to uncertainties related to convective mixing and lightning parameterizations (e.g. Doherty et al., 2005). At mid- and high latitudes, the UCI CTM model overestimates ozone while there is an underestimation of ozone by p-TOMCAT in the lower troposphere in these regions. As model validation is beyond the scope of this study, interested readers are refered to e.g. van Noije et al. (2006), Shindell et al. (2006) and Dentener et al. (2006) for evaluations of NO$_2$ columns, CO distributions and deposition budgets, respectively. When interpreting the comparison in Fig. A1, one should be aware that the Logan data are mainly from sondes launched at northern midlatitudes, hence

the observations may not be as representative in the tropics and in the Southern Hemisphere. Additionally, the observations are collected from the period 1980–1993, while the models have used emissions from year 2000 and meteorological data from 2003. Nevertheless, Stevenson et al. (2006) found that there have only been minor ozone trends between the Logan data period and year 2000, suggesting that comparisons with Logan data are still meaningful. All in all, we can conclude that the six models are capable of representing atmospheric ozone, and the ensemble mean provides a robust result as individual model errors tend to counterbalance.
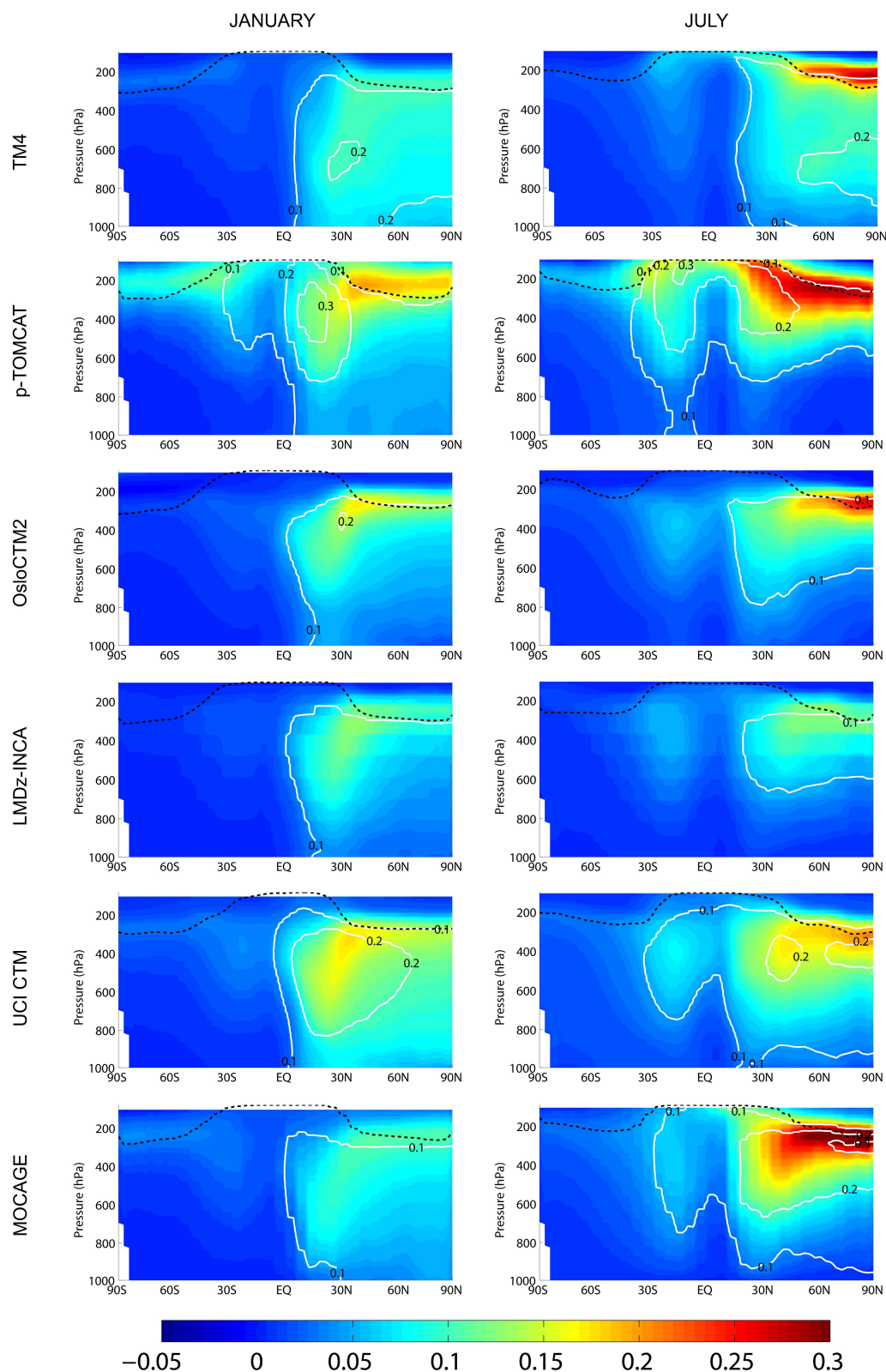
Fig. B1. Zonal mean perturbations of ozone (Δppbv) during January (left) and July (right) for the 2050 B1 scenario, due to a 5 % perturbation of aircraft emissions (simulations BASE – AIR). Solid contour lines show the change relative to the BASE simulation while the dashed line indicates the tropopause.

Fig. B2. Same as Fig. B1, but due to a 5 % perturbation of ship emissions (BASE – SHIP).

Table B4. Same as Table B3, but due to emissions from shipping.

	TM4				p-TOMCAT				OsloCTM2			
	O_3	CH_4	$O_{3(CH_4)}$	total	O_3	CH_4	$O_{3(CH_4)}$	total	O_3	CH_4	$O_{3(CH_4)}$	total
2025B1	23.6	−42.6	−15.6	−34.6	19.2	−35.5	−13.0	−29.2	33.9	−40.2	−14.7	−21.0
2050B1	26.9	−45.7	−16.7	−35.5	20.0	−37.2	−13.6	−30.8	35.5	−43.2	−15.8	−23.5

	LMDz-INCA				UCI CTM				MOCAGE			
	O_3	CH_4	$O_{3(CH_4)}$	total	O_3	CH_4	$O_{3(CH_4)}$	total	O_3	CH_4	$O_{3(CH_4)}$	total
2025B1	18.6	−34.1	−12.4	−28.0	33.3	−41.5	−15.2	−23.4	13.3	−33.2	−12.1	−32.0
2050B1	19.6	−36.7	−13.4	−30.4	36.6	−47.2	−17.3	−27.9	12.5	−35.9	−13.1	−36.5

Appendix B

Results from individual models

Individual model results are shown for the 2050 B1 scenario as zonal mean ozone perturbations for AIR and SHIP in Fig. B1 and Fig. B2, respectively. Relative changes in methane lifetimes are listed in Tables B1–B2, and RF calculations are given in Tables B3–B4.

References

ACARE: Strategic Research Agenda; Advisory Council for Aeronautics Research in Europe, Brussels, 2002.

Andreae, M. O. and Merlet, P.: Emission of trace gases and aerosols from biomass burning, Global Biogeochem. Cy., 15, 955–966, 2001.

Balkanski, Y., Myhre, G., Gauss, M., Rädel, G., Highwood, E. J., and Shine, K. P.: Direct radiative effect of aerosols emitted by transport: from road, shipping and aviation, Atmos. Chem. Phys., 10, 4477–4489, doi:10.5194/acp-10-4477-2010, 2010.

Bechtold, P., Bazile, E., Guichard, F., Mascart, P., and Richard, E.: A mass-flux convection scheme for regional and global models, Q. J. Roy. Meteorol. Soc., 127, 869–886, 2001.

Berntsen, T. K., Isaksen, I. S. A., Myhre, G., Fuglestvedt, J. S., Stordal, F., Larsen, T. A., Freckleton, R. S., and Shine, K. P.: Effects of anthropogenic emissions on tropospheric ozone and its radiative forcing, J. Geophys. Res.-Atmos., 102, 28101–28126, 1997.

Berntsen, T. K., Fuglestvedt, J. S., Joshi, M. M., Shine, K. P., Stuber, N., Ponater, M., Sausen, R., Hauglustaine, D. A., and Li, L.: Response of climate to regional emissions of ozone precursors: sensitivities and warming potentials, Tellus B, 57, 283–304, 2005.

Bian, H. S. and Prather, M. J.: Fast-J2: Accurate simulation of stratospheric photolysis in global chemical models, J. Atmos. Chem., 41, 281–296, doi:10.1023/a:1014980619462, 2002.

Borken, J., Steller, H., Meretei, T., and Vanhove, F.: Global and country inventory of road passenger and freight transportation - Fuel consumption and emissions of air pollutants in year 2000, Transp. Res. Record, 2011, 127–136, doi:10.3141/2011-14, 2007.

Brasseur, G. P., Muller, J. F., and Granier, C.: Atmospheric impact of NOx emissions by subsonic aircraft: A three-dimensional model study, J. Geophys. Res.-Atmos., 101, 1423–1428, 1996.

Burkhardt, U. and Karcher, B.: Global radiative forcing from contrail cirrus, Nat. Clim. Chang., 1, 54–58, doi:10.1038/nclimate1068, 2011.

Cariolle, D., Caro, D., Paoli, R., Hauglustaine, D. A., Cuenot, B., Cozic, A., and Paugam, R.: Parameterization of plume chemistry into large-scale atmospheric models: Application to aircraft NOx emissions, J. Geophys. Res.-Atmos., 114, D19302, doi:10.1029/2009jd011873, 2009.

Carver, G. D. and Stott, P. A.: IMPACT: an implicit time integration scheme for chemical species and families, Ann. Geophys.-Atmos. Hydrospheres Space Sci., 18, 337–346, 2000.

Carver, G. D., Brown, P. D., and Wild, O.: The ASAD atmospheric chemistry integration package and chemical reaction database, Comput. Phys. Commun., 105, 197–215, 1997.

Corbett, J. J. and Koehler, H. W.: Updated emissions from ocean shipping, J. Geophys. Res.-Atmos., 108, 4650–4665, doi:10.1029/2003jd003751, 2003.

Crassier, V., Suhre, K., Tulet, P., and Rosset, R.: Development of a reduced chemical scheme for use in mesoscale meteorological models, Atmos. Environ., 34, 2633–2644, doi:10.1016/s1352-2310(99)00480-x, 2000.

Crutzen, P. J.: Role of the tropics in atmospheric chemistry, in: The Geophysiology of Amazonia, edited by: Dickinson, R. E., John Wiley, New York, 107–130, 1987.

Dalsøren, S. B. and Isaksen, I. S. A.: CTM study of changes in tropospheric hydroxyl distribution 1990-2001 and its impact on methane, Geophys. Res. Lett., 33, L23811, doi:10.1029/2006gl027295, 2006.

Dalsøren, S. B., Eide, M. S., Endresen, Ø., Mjelde, A., Gravir, G., and Isaksen, I. S. A.: Update on emissions and environmental impacts from the international fleet of ships: the contribution from major ship types and ports, Atmos. Chem. Phys., 9, 2171–2194, doi:10.5194/acp-9-2171-2009, 2009.

Dalsøren, S. B., Eide, M. S., Myhre, G., Endresen, O., Isaksen, I. S. A., and Fuglestvedt, J. S.: Impacts of the Large Increase in International Ship Traffic 2000–2007 on Tropospheric Ozone and Methane, Environ. Sci. Technol., 44, 2482–2489, doi:10.1021/es902628e, 2010.

Danilin, M. Y., Fahey, D. W., Schumann, U., Prather, M. J., Penner, J. E., Ko, M. K. W., Weisenstein, D. K., Jackman, C. H., Pitari, G., Kohler, I., Sausen, R., Weaver, C. J., Douglass, A. R., Connell, P. S., Kinnison, D. E., Dentener, F. J., Fleming, E. L., Berntsen, T. K., Isaksen, I. S. A., Haywood, J. M., and Karcher, B.: Aviation fuel tracer simulation: Model intercomparison and implications, Geophys. Res. Lett., 25, 3947–3950, 1998.

Dentener, F., Peters, W., Krol, M., van Weele, M., Bergamaschi, P., and Lelieveld, J.: Interannual variability and trend of CH_4 lifetime as a measure for OH changes in the 1979–1993 time period, J. Geophys. Res.-Atmos., 108, 4442, doi:10.1029/2002jd002916, 2003.

Dentener, F., Drevet, J., Lamarque, J. F., Bey, I., Eickhout, B., Fiore, A. M., Hauglustaine, D., Horowitz, L. W., Krol, M., Kulshrestha, U. C., Lawrence, M., Galy-Lacaux, C., Rast, S., Shindell, D., Stevenson, D., Van Noije, T., Atherton, C., Bell, N., Bergman, D., Butler, T., Cofala, J., Collins, B., Doherty, R., Ellingsen, K., Galloway, J., Gauss, M., Montanaro, V., Muller, J. F., Pitari, G., Rodriguez, J., Sanderson, M., Solmon, F., Strahan, S., Schultz, M., Sudo, K., Szopa, S., and Wild, O.: Nitrogen and sulfur deposition on regional and global scales: A multimodel evaluation, Global Biogeochem. Cy., 20, GB4003, doi:10.1029/2005gb002672, 2006.

Doherty, R. M., Stevenson, D. S., Collins, W. J., and Sanderson, M. G.: Influence of convective transport on tropospheric ozone and its precursors in a chemistry-climate model, Atmos. Chem. Phys., 5, 3205–3218, doi:10.5194/acp-5-3205-2005, 2005.

Duncan, B. N. and Logan, J. A.: Model analysis of the factors regulating the trends and variability of carbon monoxide between 1988 and 1997, Atmos. Chem. Phys., 8, 7389–7403, doi:10.5194/acp-8-7389-2008, 2008.

Eide, M. S., Endresen, O., Mjelde, A., Mangset, L. E., and Gravir, G.: Ship emissions of the future. Technical Report No 2007-1325, Det Norske Veritas, Høvik, Norway, 2007.

Emanuel, K. A.: A scheme for representing cumulus convection in large-scale models, J. Atmos. Sci., 48, 2313–2335, 1991.

Emanuel, K. A.: A cumulus representation based on the episodic mixing model: the importance of mixing and microphysics in predicting humidity, AMS Meteorol. Monogr., 24, 185–192, 1993.

Endresen, O., Sorgard, E., Sundet, J. K., Dalsøren, S. B., Isaksen, I. S. A., Berglen, T. F., and Gravir, G.: Emission from international sea transportation and environmental impact, J. Geophys. Res.-Atmos., 108, 4560, doi:10.1029/2002jd002898, 2003.

Endresen, O., Sorgard, E., Behrens, H. L., Brett, P. O., and Isaksen, I. S. A.: A historical reconstruction of ships' fuel consumption and emissions, J. Geophys. Res.-Atmos., 112, D12301, doi:10.1029/2006jd007630, 2007.

Eyring, V., Kohler, H. W., Lauer, A., and Lemper, B.: Emissions from international shipping: 2. Impact of future technologies on scenarios until 2050, J. Geophys. Res.-Atmos., 110, D17306, doi:10.1029/2004jd005620, 2005.

Eyring, V., Stevenson, D. S., Lauer, A., Dentener, F. J., Butler, T., Collins, W. J., Ellingsen, K., Gauss, M., Hauglustaine, D. A., Isaksen, I. S. A., Lawrence, M. G., Richter, A., Rodriguez, J. M., Sanderson, M., Strahan, S. E., Sudo, K., Szopa, S., van Noije, T. P. C., and Wild, O.: Multi-model simulations of the impact of international shipping on Atmospheric Chemistry and Climate in 2000 and 2030, Atmos. Chem. Phys., 7, 757–780, doi:10.5194/acp-7-757-2007, 2007.

Eyring, V., Isaksen, I. S. A., Berntsen, T., Collins, W. J., Corbett, J. J., Endresen, O., Grainger, R. G., Moldanova, J., Schlager, H., and Stevenson, D. S.: Transport impacts on atmosphere and climate: Shipping, Atmos. Environ., 44, 4735–4771, doi:10.1016/j.atmosenv.2009.04.059, 2010.

Folberth, G. A., Hauglustaine, D. A., Lathière, J., and Brocheton, F.: Interactive chemistry in the Laboratoire de Mtorologie Dynamique general circulation model: model description and impact analysis of biogenic hydrocarbons on tropospheric chemistry, Atmos. Chem. Phys., 6, 2273–2319, doi:10.5194/acp-6-2273-2006, 2006.

Fuglestvedt, J., Berntsen, T., Myhre, G., Rypdal, K., and Skeie, R. B.: Climate forcing from the transport sectors, P. Natl. Acad. Sci. USA, 105, 454–458, doi:10.1073/pnas.0702958104, 2008.

Gauss, M., Isaksen, I. S. A., Wong, S., and Wang, W. C.: Impact of H_2O emissions from cryoplanes and kerosene aircraft on the atmosphere, J. Geophys. Res.-Atmos., 108, 4304, doi:10.1029/2002jd002623, 2003.

Gauss, M., Isaksen, I. S. A., Lee, D. S., and Søvde, O. A.: Impact of aircraft NO_x emissions on the atmosphere – trade-offs to reduce the impact, Atmos. Chem. Phys., 6, 1529–1548, doi:10.5194/acp-6-1529-2006, 2006.

Grewe, V. and Stenke, A.: AirClim: an efficient tool for climate evaluation of aircraft technology, Atmos. Chem. Phys., 8, 4621–4639, doi:10.5194/acp-8-4621-2008, 2008.

Grewe, V., Dameris, M., Hein, R., Kohler, I., and Sausen, R.: Impact of future subsonic aircraft NOx emissions on the atmospheric composition, Geophys. Res. Lett., 26, 47–50, 1999.

Grewe, V., Stenke, A., Ponater, M., Sausen, R., Pitari, G., Iachetti, D., Rogers, H., Dessens, O., Pyle, J., Isaksen, I. S. A., Gulstad, L., Søvde, O. A., Marizy, C., and Pascuillo, E.: Climate impact of supersonic air traffic: an approach to optimize a potential future supersonic fleet results from the EU-project SCENIC, Atmos. Chem. Phys., 7, 5129–5145, doi:10.5194/acp-7-5129-2007, 2007.

Grewe, V., Tsati, E., and Hoor, P.: On the attribution of contributions of atmospheric trace gases to emissions in atmospheric model applications, Geosci. Model Dev., 3, 487–499, doi:10.5194/gmd-3-487-2010, 2010.

Grooß, J. U., Bruhl, C., and Peter, T.: Impact of aircraft emissions on tropospheric and stratospheric ozone. Part I: Chemistry and 2-D model results, Atmos. Environ., 32, 3173–3184, 1998.

Hansen, J., Sato, M., and Ruedy, R.: Radiative forcing and climate response, J. Geophys. Res.-Atmos., 102, 6831–6864, 1997.

Hauglustaine, D. A., Hourdin, F., Jourdain, L., Filiberti, M. A., Walters, S., Lamarque, J. F., and Holland, E. A.: Interactive chemistry in the Laboratoire de Meteorologie Dynamique general circulation model: Description and background tropospheric

chemistry evaluation, J. Geophys. Res.-Atmos., 109, D04314, doi:10.1029/2003jd003957, 2004.

Hesstvedt, E., Hov, O., and Isaksen, I. S. A.: Quasi-steady-state approximations in air pollution modeling - Comparison of two numerical schemes for oxidant prediction, Int. J. Chem. Kinet., 10, 971–994, 1978.

Hidalgo, H. and Crutzen, P. J.: Tropospheric and stratospheric composition perturbed by NO_x emissions of high-altitude aircraft, J. Geophys. Res.-Oceans, 82, 5833–5866, 1977.

Hoor, P., Borken-Kleefeld, J., Caro, D., Dessens, O., Endresen, O., Gauss, M., Grewe, V., Hauglustaine, D., Isaksen, I. S. A., Jöckel, P., Lelieveld, J., Myhre, G., Meijer, E., Olivie, D., Prather, M., Schnadt Poberaj, C., Shine, K. P., Staehelin, J., Tang, Q., van Aardenne, J., van Velthoven, P., and Sausen, R.: The impact of traffic emissions on atmospheric ozone and OH: results from QUANTIFY, Atmos. Chem. Phys., 9, 3113–3136, doi:10.5194/acp-9-3113-2009, 2009.

Hourdin, F. and Armengaud, A.: The use of finite-volume methods for atmospheric advection of trace species. Part I: Test of various formulations in a general circulation model, Mon. Weather Rev., 127, 822–837, 1999.

Houweling, S., Dentener, F., and Lelieveld, J.: The impact of non-methane hydrocarbon compounds on tropospheric photochemistry, J. Geophys. Res.-Atmos., 103, 10673–10696, 1998.

Hsu, J., Prather, M. J., and Wild, O.: Diagnosing the stratosphere-to-troposphere flux of ozone in a chemistry transport model, J. Geophys. Res.-Atmos., 110, D19305, doi:10.1029/2005jd006045, 2005.

Huszar, P., Cariolle, D., Paoli, R., Halenka, T., Belda, M., Schlager, H., Miksovsky, J., and Pisoft, P.: Modeling the regional impact of ship emissions on NO_x and ozone levels over the Eastern Atlantic and Western Europe using ship plume parameterization, Atmos. Chem. Phys., 10, 6645–6660, doi:10.5194/acp-10-6645-2010, 2010.

IPCC: Aviation and the Global Atmosphere, edited by: Penner, J. E., Lister, D. H., Griggs, D. J., Dokken, D. J., and McFarland, M., Cambridge University Press, Cambridge, United Kingdom and New York, NY, USA, 1999.

IPCC: Climate Change 2001: The Scientific Basis. Contribution of Working Group I to the Third Assessment Report of the Intergovernmental Panel on Climate Change, edited by: Houghton, J. T., Ding, Y., Griggs, D. J., Noguer, M., van der Linden, P. J., Dai, X., Maskell, K., and Johnson, C. A., Cambridge University Press, Cambridge, United Kingdom and New York, NY, USA., 881 pp., 2001.

Isaksen, I. S. A. and Dalsøren, S. B.: Getting a Better Estimate of an Atmospheric Radical, Science, 331, 38–39, doi:10.1126/science.1199773, 2011.

Jöckel, P., Tost, H., Pozzer, A., Brühl, C., Buchholz, J., Ganzeveld, L., Hoor, P., Kerkweg, A., Lawrence, M. G., Sander, R., Steil, B., Stiller, G., Tanarhte, M., Taraborrelli, D., van Aardenne, J., and Lelieveld, J.: The atmospheric chemistry general circulation model ECHAM5/MESSy1: consistent simulation of ozone from the surface to the mesosphere, Atmos. Chem. Phys., 6, 5067–5104, doi:10.5194/acp-6-5067-2006, 2006.

Johnson, C., Henshaw, J., and McInnes, G.: Impact of aircraft and surface emissions of nitrogen-oxides on tropospheric ozone and global warming, Nature, 355, 69–71, 1992.

Koffi, B., Szopa, S., Cozic, A., Hauglustaine, D., and van

Velthoven, P.: Present and future impact of aircraft, road traffic and shipping emissions on global tropospheric ozone, Atmos. Chem. Phys., 10, 11681–11705, doi:10.5194/acp-10-11681-2010, 2010.

Kraabøl, A. G., Berntsen, T. K., Sundet, J. K., and Stordal, F.: Impacts of NO_x emissions from subsonic aircraft in a global three-dimensional chemistry transport model including plume processes, J. Geophys. Res.-Atmos., 107, 4655, doi:10.1029/2001jd001019, 2002.

Lacis, A. A., Wuebbles, D. J., and Logan, J. A.: Radiative forcing of climate by changes in the vertical-distribution of ozone, J. Geophys. Res.-Atmos., 95, 9971–9981, 1990.

Law, K. S., Plantevin, P. H., Shallcross, D. E., Rogers, H. L., Pyle, J. A., Grouhel, C., Thouret, V., and Marenco, A.: Evaluation of modeled O-3 using Measurement of Ozone by Airbus In-Service Aircraft (MOZAIC) data, J. Geophys. Res.-Atmos., 103, 25721–25737, 1998.

Law, K. S., Plantevin, P. H., Thouret, V., Marenco, A., Asman, W. A. H., Lawrence, M., Crutzen, P. J., Muller, J. F., Hauglustaine, D. A., and Kanakidou, M.: Comparison between global chemistry transport model results and Measurement of Ozone and Water Vapor by Airbus In-Service Aircraft (MOZAIC) data, J. Geophys. Res.-Atmos., 105, 1503–1525, 2000.

Lawrence, M. G. and Crutzen, P. J.: Influence of NO_x emissions from ships on tropospheric photochemistry and climate, Nature, 402, 167–170, 1999.

Le Treut, H., Forichon, M., Boucher, O., and Li, Z. X.: Sulfate aerosol indirect effect and CO2 greenhouse forcing: Equilibrium response of the LMD GCM and associated cloud feedbacks, J. Clim., 11, 1673–1684, 1998.

Lee, D. S., Fahey, D. W., Forster, P. M., Newton, P. J., Wit, R. C. N., Lim, L. L., Owen, B., and Sausen, R.: Aviation and global climate change in the 21st century, Atmos. Environ., 43, 3520–3537, doi:10.1016/j.atmosenv.2009.04.024, 2009.

Lee, D. S., Pitari, G., Grewe, V., Gierens, K., Penner, J. E., Petzold, A., Prather, M. J., Schumann, U., Bais, A., Berntsen, T., Iachetti, D., Lim, L. L., and Sausen, R.: Transport impacts on atmosphere and climate: Aviation, Atmos. Environ., 44, 4678–4734, doi:10.1016/j.atmosenv.2009.06.005, 2010.

Lefèvre, F., Brasseur, G. P., Folkins, I., Smith, A. K., and Simon, P.: Chemistry of the 1991-1992 stratospheric winter: Three-dimensional model simulations, J. Geophys. Res., 99, 8183–8195, doi:10.1029/93jd03476, 1994.

Lelieveld, J., Peters, W., Dentener, F. J., and Krol, M. C.: Stability of tropospheric hydroxyl chemistry, J. Geophys. Res.-Atmos., 107, 4715, doi:10.1029/2002jd002272, 2002.

Lelieveld, J., Brenninkmeijer, C. A. M., Joeckel, P., Isaksen, I. S. A., Krol, M. C., Mak, J. E., Dlugokencky, E., Montzka, S. A., Novelli, P. C., Peters, W., and Tans, P. P.: New Directions: Watching over tropospheric hydroxyl (OH), Atmos. Environ., 40, 5741–5743, doi:10.1016/j.atmosenv.2006.04.008, 2006.

Logan, J. A.: An analysis of ozonesonde data for the troposphere: Recommendations for testing 3-D models and development of a gridded climatology for tropospheric ozone, J. Geophys. Res., 104, 16115–16149, doi:10.1029/1998jd100096, 1999.

Luo, B., Carslaw, K. S., Peter, T., and Clegg, S. L.: Vapour pressures of $H_2SO_4/HNO_3/HCl/HBr/H_2O$ solutions to low stratospheric temperatures, Geophys. Res. Lett., 22, 247–250, doi:10.1029/94gl02988, 1995.

Meijer, E. W., van Velthoven, P. F. J., Brunner, D. W., Huntrieser, H., and Kelder, H.: Improvement and evaluation of the parameterisation of nitrogen oxide production by lightning, Phys. Chem. Earth Pt. C-Solar-Terr. Planet. Sci., 26, 577–583, 2001.

Montzka, S. A., Krol, M., Dlugokencky, E., Hall, B., Jöckel, P., and Lelieveld, J.: Small Interannual Variability of Global Atmospheric Hydroxyl, Science, 331, 67–69, doi:10.1126/science.1197640, 2011.

Myhre, G., Karlsdottir, S., Isaksen, I. S. A., and Stordal, F.: Radiative forcing due to changes in tropospheric ozone in the period 1980 to 1996, J. Geophys. Res.-Atmos., 105, 28935–28942, 2000.

Myhre, G., Nilsen, J. S., Gulstad, L., Shine, K. P., Rognerud, B., and Isaksen, I. S. A.: Radiative forcing due to stratospheric water vapour from CH_4 oxidation, Geophys. Res. Lett., 34, L01807, doi:10.1029/2006gl027472, 2007.

Myhre, G., Shine, K. P., Rädel, G., Gauss, M., Isaksen, I. S. A., Tang, Q., Prather, M. J., Williams, J. E., van Velthoven, P., Dessens, O., Koffi, B., Szopa, S., Hoor, P., Grewe, V., Borken-Kleefeld, J., Berntsen, T. K., and Fuglestvedt, J. S.: Radiative forcing due to changes in ozone and methane caused by the transport sector, Atmos. Environ., 45, 387–394, doi:10.1016/j.atmosenv.2010.10.001, 2011.

Nakicenovic, N., Davidson, O., Davis, G., Grübler, A., Kram, T., La Rovere, E. L., Metz, B., Morita, T., Pepper, W., Pitcher, H., Sankovski, A., Shukla, P., Swart, R., Watson, R., and Dadi, Z.: Special Report on Emissions Scenarios, Cambridge University Press, Cambridge, 599 pp., 2000.

O'Connor, F. M., Carver, G. D., Savage, N. H., Pyle, J. A., Methven, J., Arnold, S. R., Dewey, K., and Kent, J.: Comparison and visualisation of high-resolution transport modelling with aircraft measurements, Atmos. Sci. Lett., 6, 164–170, doi:10.1002/asl.111, 2005.

Olivier, J. G. J., Van Aardenne, J. A., Dentener, F., Ganzeveld, L., and Peters, J. A. H. W.: Recent trends in global greenhouse gas emissions: regional trends and spatial distribution of key sources, in: Non-CO2 Greenhouse Gases (NCGG-4), Millpress, Rotterdam, 325–330, 2005.

Owen, B., Lee, D. S., and Lim, L.: Flying into the Future: Aviation Emissions Scenarios to 2050, Environ. Sci. Technol., 44, 2255-2260, doi:10.1021/es902530z, 2010.

Prather, M. J.: Numerical advection by conservation of 2nd-order moments, J. Geophys. Res.-Atmos., 91, 6671–6681, 1986.

Prather, M. J. and Hsu, J.: Coupling of Nitrous Oxide and Methane by Global Atmospheric Chemistry, Science, 330, 952–954, doi:10.1126/science.1196285, 2010.

Prather, M. J., Zhu, X., Tang, Q., Hsu, J., and Neu, J. L.: An atmospheric chemist in search of the tropopause, J. Geophys. Res., 116, D04306, doi:10.1029/2010JD014939, 2011.

Price, C. and Rind, D.: A simple lightning parameterization for calculating global lightning distributions, J. Geophys. Res.-Atmos., 97, 9919–9933, 1992.

Ramanathan, V. and Dickinson, R. E.: Role of stratospheric ozone in the zonal and seasonal radiative energy-balance of the Earth-troposphere system, J. Atmos. Sci., 36, 1084–1104, 1979.

Rogers, H., Teyssèdre, H., Pitari, G., Grewe, V., van Velthoven, P., and Sundet, J.: Model intercomparison of the transport of aircraft-like emissions from sub- and supersonic aircraft, Meteorol. Z., 11, 151–159, doi:10.1127/0941-2948/2002/0011-0151, 2002.

Russell, G. L. and Lerner, J. A.: A new finite-differencing scheme for the tracer transport-equation, J. Appl. Meteorol., 20, 1483–1498, 1981.

Sander, S. P., Orkin, V. L., Kurylo, M. J., Golden, D. M., Barker, J. R., Huie, R. E., Kolb, C. E., Abbatt, J. P. D., Friedl, R. R., Burkholder, J. B., Moortgat, G. K., and Wine, P. H.: Chemical kinetics and photochemical data for use in atmospheric studies, JPL Publication 06–2, NASA/JPL, Jet Propulsion Laboratory, California Institute of Technology, Pasadena, California, Evaluation Number 15, 2006.

Sausen, R., Isaksen, I., Grewe, V., Hauglustaine, D., Lee, D. S., Myhre, G., Kohler, M. O., Pitari, G., Schumann, U., Stordal, F., and Zerefos, C.: Aviation radiative forcing in 2000: An update on IPCC (1999), Meteorol. Z., 14, 555–561, doi:10.1127/0941-2948/2005/0049, 2005.

Savage, N. H., Law, K. S., Pyle, J. A., Richter, A., Nüß, H., and Burrows, J. P.: Using GOME NO_2 satellite data to examine regional differences in TOMCAT model performance, Atmos. Chem. Phys., 4, 1895–1912, doi:10.5194/acp-4-1895-2004, 2004.

Schnadt Poberaj, C., Staehelin, J., Bintania, R., van Velthoven, P., Dessens, O., Gauss, M., Isaksen, I. S. A., Grewe, V., Jöckel, P., Hoor, P., Koffi, B., Hauglustaine, D., and Olivié, D.: QUANTIFY model evaluation of global chemistry models: carbon monoxide, Proceedings of the 2nd International Conference on Transport, Atmosphere and Climate, DLR Forschungsbericht 2010-10, ISSN 1434-8454,163-168, 2010,

Schumann, U.: The impact of nitrogen oxides emissions from aircraft upon the atmosphere at flight altitudes - Results from the AERONOX project, Atmos. Environ., 31, 1723–1733, 1997.

Schumann, U. and Huntrieser, H.: The global lightning-induced nitrogen oxides source, Atmos. Chem. Phys., 7, 3823–3907, doi:10.5194/acp-7-3823-2007, 2007.

Schumann, U., Schlager, H., Arnold, F., Ovarlez, J., Kelder, H., Hov, O., Hayman, G., Isaksen, I. S. A., Staehelin, J., and Whitefield, P. D.: Pollution from aircraft emissions in the North Atlantic flight corridor: Overview on the POLINAT projects, J. Geophys. Res.-Atmos., 105, 3605–3631, 2000.

Shindell, D. T., Faluvegi, G., Bell, N., and Schmidt, G. A.: An emissions-based view of climate forcing by methane and tropospheric ozone, Geophys. Res. Lett., 32, L04803, doi:10.1029/2004gl021900, 2005.

Shindell, D. T., Faluvegi, G., Stevenson, D. S., Krol, M. C., Emmons, L. K., Lamarque, J. F., Petron, G., Dentener, F. J., Ellingsen, K., Schultz, M. G., Wild, O., Amann, M., Atherton, C. S., Bergmann, D. J., Bey, I., Butler, T., Cofala, J., Collins, W. J., Derwent, R. G., Doherty, R. M., Drevet, J., Eskes, H. J., Fiore, A. M., Gauss, M., Hauglustaine, D. A., Horowitz, L. W., Isaksen, I. S. A., Lawrence, M. G., Montanaro, V., Muller, J. F., Pitari, G., Prather, M. J., Pyle, J. A., Rast, S., Rodriguez, J. M., Sanderson, M. G., Savage, N. H., Strahan, S. E., Sudo, K., Szopa, S., Unger, N., van Noije, T. P. C., and Zeng, G.: Multimodel simulations of carbon monoxide: Comparison with observations and projected near-future changes, J. Geophys. Res.-Atmos., 111, D19306, doi:10.1029/2006jd007100, 2006.

Skeie, R. B., Fuglestvedt, J., Berntsen, T., Lund, M. T., Myhre, G., and Rypdal, K.: Global temperature change from the transport sectors: Historical development and future scenarios, Atmos.

Environ., 43, 6260–6270, doi:10.1016/j.atmosenv.2009.05.025, 2009.

Søvde, O. A., Gauss, M., Isaksen, I. S. A., Pitari, G., and Marizy, C.: Aircraft pollution – a futuristic view, Atmos. Chem. Phys., 7, 3621–3632, doi:10.5194/acp-7-3621-2007, 2007.

Søvde, O. A., Gauss, M., Smyshlyaev, S. P., and Isaksen, I. S. A.: Evaluation of the chemical transport model Oslo CTM2 with focus on arctic winter ozone depletion, J. Geophys. Res.-Atmos., 113, D09304, doi:10.1029/2007jd009240, 2008.

Søvde, O. A., Hoyle, C. R., Myhre, G., and Isaksen, I. S. A.: The HNO_3 forming branch of the $HO_2 + NO$ reaction: pre-industrial-to-present trends in atmospheric species and radiative forcings, Atmos. Chem. Phys., 11, 8929–8943, doi:10.5194/acp-11-8929-2011, 2011.

Stevenson, D. S., Doherty, R. M., Sanderson, M. G., Collins, W. J., Johnson, C. E., and Derwent, R. G.: Radiative forcing from aircraft NOx emissions: Mechanisms and seasonal dependence, J. Geophys. Res.-Atmos., 109, D17307, doi:10.1029/2004jd004759, 2004.

Stevenson, D. S., Dentener, F. J., Schultz, M. G., Ellingsen, K., van Noije, T. P. C., Wild, O., Zeng, G., Amann, M., Atherton, C. S., Bell, N., Bergmann, D. J., Bey, I., Butler, T., Cofala, J., Collins, W. J., Derwent, R. G., Doherty, R. M., Drevet, J., Eskes, H. J., Fiore, A. M., Gauss, M., Hauglustaine, D. A., Horowitz, L. W., Isaksen, I. S. A., Krol, M. C., Lamarque, J. F., Lawrence, M. G., Montanaro, V., Muller, J. F., Pitari, G., Prather, M. J., Pyle, J. A., Rast, S., Rodriguez, J. M., Sanderson, M. G., Savage, N. H., Shindell, D. T., Strahan, S. E., Sudo, K., and Szopa, S.: Multimodel ensemble simulations of present-day and near-future tropospheric ozone, J. Geophys. Res.-Atmos., 111, D08301, doi:10.1029/2005jd006338, 2006.

Stockwell, W. R., Kirchner, F., Kuhn, M., and Seefeld, S.: A new mechanism for regional atmospheric chemistry modeling, J. Geophys. Res., 102, 25847–25879, doi:10.1029/97jd00849, 1997.

Tang, Q. and Prather, M. J.: Correlating tropospheric column ozone with tropopause folds: the Aura-OMI satellite data, Atmos. Chem. Phys., 10, 9681–9688, doi:10.5194/acp-10-9681-2010, 2010.

Tang, Q., Prather, M. J., and Hsu, J.: Stratosphere-troposphere exchange ozone flux related to deep convection, Geophys. Res. Lett., 38, L03806, doi:10.1029/2010gl046039, 2011.

Teyssèdre, H., Michou, M., Clark, H. L., Josse, B., Karcher, F., Olivié, D., Peuch, V.-H., Saint-Martin, D., Cariolle, D., Attié, J.-L., Nédélec, P., Ricaud, P., Thouret, V., van der A, R. J., Volz-Thomas, A., and Chéroux, F.: A new tropospheric and stratospheric Chemistry and Transport Model MOCAGE-Climat for multi-year studies: evaluation of the present-day climatology and sensitivity to surface processes, Atmos. Chem. Phys., 7, 5815–5860, doi:10.5194/acp-7-5815-2007, 2007.

Tiedtke, M.: A comprehensive mass flux scheme for cumulus parameterization in large-scale models, Mon. Weather Rev., 117, 1779–1800, 1989.

Uherek, E., Halenka, T., Borken-Kleefeld, J., Balkanski, Y., Berntsen, T., Borrego, C., Gauss, M., Hoor, P., Juda-Rezler, K., Lelieveld, J., Melas, D., Rypdal, K., and Schmid, S.: Transport impacts on atmosphere and climate: Land transport, Atmos. Environ., 44, 4772–4816, doi:10.1016/j.atmosenv.2010.01.002, 2010.

van Aardenne, J. A., Dentener, F. D., Olivier, J. G. J., Peters, J. A. H. W., and Ganzeveld, L. N.: The EDGAR 3.2 Fast Track 2000 dataset (32FT2000), available at: http://themasites.pbl.nl/images/Description_of_EDGAR_32FT2000(v8)_tcm61-46462.pdf, Joint Research Center, Institute for Environment and Sustainability (JRC-IES), Climate Change Unit, Ispra, Italy, 2005.

van der Werf, G. R., Randerson, J. T., Giglio, L., Collatz, G. J., Kasibhatla, P. S., and Arellano Jr., A. F.: Interannual variability in global biomass burning emissions from 1997 to 2004, Atmos. Chem. Phys., 6, 3423–3441, doi:10.5194/acp-6-3423-2006, 2006.

Van Leer, B.: Towards the ultimate conservative difference scheme. IV. A new approach to numerical convection, J. Comput. Phys., 23, 276–299, doi:10.1016/0021-9991(77)90095-x, 1977.

van Noije, T. P. C., Eskes, H. J., Dentener, F. J., Stevenson, D. S., Ellingsen, K., Schultz, M. G., Wild, O., Amann, M., Atherton, C. S., Bergmann, D. J., Bey, I., Boersma, K. F., Butler, T., Cofala, J., Drevet, J., Fiore, A. M., Gauss, M., Hauglustaine, D. A., Horowitz, L. W., Isaksen, I. S. A., Krol, M. C., Lamarque, J.-F., Lawrence, M. G., Martin, R. V., Montanaro, V., Müller, J.-F., Pitari, G., Prather, M. J., Pyle, J. A., Richter, A., Rodriguez, J. M., Savage, N. H., Strahan, S. E., Sudo, K., Szopa, S., and van Roozendael, M.: Multi-model ensemble simulations of tropospheric NO2 compared with GOME retrievals for the year 2000, Atmos. Chem. Phys., 6, 2943–2979, doi:10.5194/acp-6-2943-2006, 2006.

Wang, W. C. and Sze, N. D.: Coupled effects of atmospheric N_2O and O_3 on the Earth's climate, Nature, 286, 589–590, 1980.

Wild, O., Zhu, X., and Prather, M. J.: Fast-j: Accurate simulation of in- and below-cloud photolysis in tropospheric chemical models, J. Atmos. Chem., 37, 245–282, 2000.

Wild, O., Sundet, J. K., Prather, M. J., Isaksen, I. S. A., Akimoto, H., Browell, E. V., and Oltmans, S. J.: Chemical transport model ozone simulations for spring 2001 over the western Pacific: Comparisons with TRACE-P lidar, ozonesondes, and Total Ozone Mapping Spectrometer columns, J. Geophys. Res.-Atmos., 108, 8826, doi:10.1029/2002jd003283, 2003.

Williams, J. E. and van Noije, T. P. C.: On the updating of the modified Carbon Bond Mechanism IV for use in global Chemistry Transport Models, KNMI Scientific Report WR 2008-02, De Bilt, The Netherlands, 64 pp., 2008.

Williams, J. E., Scheele, M. P., van Velthoven, P. F. J., Thouret, V., Saunois, M., Reeves, C. E., and Cammas, J.-P.: The influence of biomass burning and transport on tropospheric composition over the tropical Atlantic Ocean and Equatorial Africa during the West African monsoon in 2006, Atmos. Chem. Phys., 10, 9797–9817, doi:10.5194/acp-10-9797-2010, 2010.

Williamson, D. L. and Rasch, P. J.: Two-dimensional semi-lagrangian transport with shape-preserving interpolation, Mon. Weather Rev., 117, 102–129, 1989.

Yurganov, L. N., Duchatelet, P., Dzhola, A. V., Edwards, D. P., Hase, F., Kramer, I., Mahieu, E., Mellqvist, J., Notholt, J., Novelli, P. C., Rockmann, A., Scheel, H. E., Schneider, M., Schulz, A., Strandberg, A., Sussmann, R., Tanimoto, H., Velazco, V., Drummond, J. R., and Gille, J. C.: Increased Northern Hemispheric carbon monoxide burden in the troposphere in 2002 and 2003 detected from the ground and from space, Atmos. Chem. Phys., 5, 563–573, doi:10.5194/acp-5-563-2005, 2005.